



**AFRL-RQ-ED-TR-2016-0025**

# **Ionic Liquid Fuels for Chemical Propulsion**

---

Stefan Schneider

Air Force Research Laboratory (AFMC)  
AFRL/RQRP  
10 E. Saturn Blvd.  
Edwards AFB, CA 93524

October 2016

In-House Interim Report

---

Distribution A: Approved for Public Release; distribution unlimited. PA No. 16565

---

**STINFO COPY**

**AIR FORCE RESEARCH LABORATORY  
AEROSPACE SYSTEMS DIRECTORATE**

**- STINFO COPY -**  
**NOTICE AND SIGNATURE PAGE**

Using Government drawings, specifications, or other data included in this document for any purpose other than Government procurement does not in any way obligate the U.S. Government. The fact that the Government formulated or supplied the drawings, specifications, or other data does not license the holder or any other person or corporation; or convey any rights or permission to manufacture, use, or sell any patented invention that may relate to them.

This report was cleared for public release by the USAF 412 Test Wing (412 TW) Public Affairs Office (PAO) and is available to the general public, including foreign nationals.

AFRL-RQ-ED-TR-2016-0025 HAS BEEN REVIEWED AND IS APPROVED FOR PUBLICATION IN ACCORDANCE WITH ASSIGNED DISTRIBUTION STATEMENT.

FOR THE DIRECTOR:

//Signature//

---

STEFAN SCHNEIDER, Ph.D.  
Program Manager

//Signature//

---

TIMOTHY A. MCKELVEY  
Chief, Propellants Branch

//Signature//

---

JOSEPH M. MABRY, Ph.D.  
Technical Advisor  
Rocket Propulsion Division

This report is published in the interest of scientific and technical information exchange, and its publication does not constitute the Government's approval or disapproval of its ideas or findings.

REPORT DOCUMENTATION PAGE				Form Approved OMB No. 0704-0188	
<p>Public reporting burden for this collection of information is estimated to average 1 hour per response, including the time for reviewing instructions, searching existing data sources, gathering and maintaining the data needed, and completing and reviewing this collection of information. Send comments regarding this burden estimate or any other aspect of this collection of information, including suggestions for reducing this burden to Department of Defense, Washington Headquarters Services, Directorate for Information Operations and Reports (0704-0188), 1215 Jefferson Davis Highway, Suite 1204, Arlington, VA 22202-4302. Respondents should be aware that notwithstanding any other provision of law, no person shall be subject to any penalty for failing to comply with a collection of information if it does not display a currently valid OMB control number. <b>PLEASE DO NOT RETURN YOUR FORM TO THE ABOVE ADDRESS.</b></p>					
1. REPORT DATE (MM/DD/YYYY) October 2016		2. REPORT TYPE In-House Interim Report		3. DATES COVERED (From - To) 10/1/2013 – 09/30/2016	
4. TITLE AND SUBTITLE Ionic Liquid Fuels for Chemical Propulsion				5a. CONTRACT NUMBER	
				5b. GRANT NUMBER	
				5c. PROGRAM ELEMENT NUMBER	
6. AUTHOR(S) Stefan Schneider				5d. PROJECT NUMBER	
				5e. TASK NUMBER	
				5f. WORK UNIT NUMBER Q0RA	
7. PERFORMING ORGANIZATION NAME(S) AND ADDRESS(ES) Air Force Research Laboratory (AFMC) AFRL/RQRP 10 E. Saturn Blvd. Edwards AFB, CA 93524				8. PERFORMING ORGANIZATION REPORT NO.  AFRL-RQ-ED-TR-2016-0025	
9. SPONSORING / MONITORING AGENCY NAME(S) AND ADDRESS(ES)  Air Force Research Laboratory (AFMC) AFRL/RQR 5 Pollux Drive Edwards AFB, CA 93524				10. SPONSOR/MONITOR'S ACRONYM(S)	
				11. SPONSOR/MONITOR'S REPORT NUMBER(S)	
12. DISTRIBUTION / AVAILABILITY STATEMENT Approved for public release; distribution unlimited					
13. SUPPLEMENTARY NOTES AFTC 412 TW PA Clearance #: 16565					
14. ABSTRACT LRIR #14RQ11COR Task I: Unfortunately, neither the cyanoborohydride approach nor the pure tetrakis-tetrahydroborate aluminate ILs discovered possess the desirable physical properties for a suitable propellant. In general, their major shortcomings still are poor liquid range and high viscosity as well as the high hydrocarbon content of the cations required to lower their melting points which severely limits propellant performance. In light of our discoveries we turned to systems simpler and higher performing than the complexed Al(BH4)4- anions. Solutions of Li-Al hydrides and LiBH4 in ethers have shown some desirable propellant properties and a variety of lithium metal hydrides are commercially available. This suggested an entry point into the coordination chemistry of lithium salts with some new high energy heterocyclic ring systems. Task II: In this work we have used a variety of complementary experimental techniques and theoretical approaches to elucidate the reaction mechanisms involved in the decomposition of energetic RTILs as a result of thermolysis, catalysis and oxidation. As our knowledge improves in these areas, it should be possible to build predictive numerical models for the accurate assessment of the performance and the state-of-health in RTIL monopropellant and bipropellant thrusters.					
15. SUBJECT TERMS Ionic liquids; energetic materials; chemical kinetics; hypergolic fuels; salts; ligands; lithium; borohydrides; density functional theory; flammability					
16. SECURITY CLASSIFICATION OF:			17. LIMITATION OF ABSTRACT  SAR	18. NUMBER OF PAGES  43	19a. NAME OF RESPONSIBLE PERSON Stefan Schneider
a. REPORT  Unclassified	b. ABSTRACT  Unclassified	c. THIS PAGE  Unclassified			19b. TELEPHONE NO (include area code)

This Page Intentionally Left Blank

## TABLE OF CONTENTS

<b>1.0</b>	<b>INTRODUCTION .....</b>	<b>1</b>
1.1.	TASK I.....	1
1.2	TASK II.....	1
<b>2.0</b>	<b>TECHNICAL SUMMARY .....</b>	<b>2</b>
2.1	TASK I.....	2
2.2	TASK II.....	16
<b>3.0</b>	<b>PUBLICATIONS .....</b>	<b>28</b>
<b>4.0</b>	<b>Appendix A: In-house Activities .....</b>	<b>32</b>
	<b>Appendix B: Technology Assists, Transitions, or Transfers .....</b>	<b>33</b>

## LIST OF FIGURES

Figure 1. Different coordination possibilities of $[\text{NCBH}_3]^-$ to $\text{ABH}$ .....	2
Figure 2. A new, doubly charged anion (calc., left; crystal structure, right) $[\text{Al}(\text{BH}_4)_2(\text{NCBH}_3)_3]^{2-}$ .....	3
Figure 3. X-ray crystal structure of isolated product showing a rare example of a hexacoordinated, triply charged aluminum anion .....	3
Figure 4. Transition states of $\text{BH}_4^- \cdot \text{H}_2\text{O}$ and $\text{BH}_3 \cdot \text{H}_2\text{O}$ .....	6
Figure 5. Energy profiles along the Intrinsic Reaction Coordinate (IRC) for the hydrolysis of the $[\text{Al}(\text{BH}_4)_4]^-$ ..	6
Figure 6. Single crystal X-ray structure of the hydrochloride 9 and 5-(hydrazino-alkyl) tetrazoles 1 .....	8
Figure 7. Modes of borohydride coordination with metal centers in solvated systems .....	9
Figure 8. Crystal Structure of $\text{Li}(\text{1,5-dimethyltetrazole})_2 \text{BH}_4$ .....	10
Figure 9. Crystal structure of $\text{Li}(\text{2,5-Dimethyltetrazole})\text{BH}_4$ .....	11
Figure 10. $^1\text{H}$ NMR of $\text{Li}_2(\text{H}_2\text{NCH}_3)_3(\text{BH}_4)_2$ .....	11
Figure 11. $^{11}\text{B}$ NMR of $\text{Li}_2(\text{H}_2\text{NCH}_3)_3(\text{BH}_4)_2$ .....	11
Figure 12. DSC of $\text{Li}_2(\text{H}_2\text{NCH}_3)_3(\text{BH}_4)_2$ .....	12
Figure 13. TGA-MS of $\text{Li}_2(\text{H}_2\text{NCH}_3)_3(\text{BH}_4)_2$ .....	12
Figure 14. Solvation by diethylenetriamine compared to the known Li-glyme-complex .....	12
Figure 15. Initial $^1\text{H}$ (left) and $^{11}\text{B}$ NMR (right) of $\text{Li}(\text{diethylenetriamine})\text{BH}_4$ .....	13
Figure 16. $^1\text{H}$ (left) and $^{11}\text{B}$ NMR (right) of $\text{Li}(\text{diethylenetriamine})\text{BH}_4$ after 2d (bottom), after 5d (top) ...	13
Figure 17. Modified test stand installed at Purdue University, Zucrow Test Facility .....	14
Figure 18. Drop test image of AFRL fuel and WFNA: Ignition within 1.1ms .....	14
Figure 19. Successful hotfire-test at Purdue University measured ISP and $\text{C}^*$ efficiency .....	15
Figure 20. Thermal decomposition mechanisms of $\text{EMIM}^+\text{SCN}^-$ , including $-\text{CH}_3$ and $-\text{CH}_2\text{CH}_3$ abstractions and S substitution at EMIM C2 evidenced by vacuum ultraviolet-time of flight mass spectrometry .....	17
Figure 21. Depiction of the diffusion-limited process in the ignition of hypergolic DCA-based ionic liquids with $\text{HNO}_3$ .....	19
Figure 22. Ignition delay time of boron nanoparticle-infused ionic liquids $\text{MAT}^+\text{DCA}^-$ and $\text{AMIM}^+\text{DCA}^-$ as a function of particle loading as determined by the evolution of $\text{CO}_2$ by rapid-scan Fourier-transform infrared spectroscopy .....	19
Figure 23. X-ray photoelectron spectrum (XPS, left) of the oxidized and protected boron nanoparticles, and scanning electron microscope image (SEM, right) of the ball milled boron nanoparticles that have been protected .....	20
Figure 24. The potential energy surface for the thermal decomposition of DNB calculated at the M06-2X/aug-cc-pVTZ level of theory .....	23
Figure 25. Typical $[\text{HONO}]$ temporal profile observed in the flow-tube reactor at 298 K .....	24
Figure 26. High pressure limit rate coefficients for the dissociation and isomerization channels of $\text{N}_2\text{H}_3 + \text{NO}_2 \rightarrow \text{N}_2\text{H}_3\text{NO}_2 \rightarrow \text{Products}$ (left) and of $\text{N}_2\text{H}_3 + \text{NO}_2 \rightarrow \text{N}_2\text{H}_3\text{ONO} \rightarrow \text{Products}$ (right) .....	25
Figure 27. MMH/NTO/He (with 60 mol% of He) flammability diagram as a function of total mixture pressure and equivalence ratio obtained by assuming rapid mixing .....	25

## LIST OF TABLES

Table 1. Energies (kcal/mol) for the reactions which form H <sub>2</sub> by hydrolysis .....	7
Table 2. Calculated free energies of acidity, $\Delta G_{acid}$ , in the gas phase and in the condensed phase by SMD-GIL and SMD (water) at the M06/6-31+G(d,p) level of theory.....	18
Table 3. Direct dynamics trajectory simulation results for H• + DNB• collisions.....	21

## LIST OF SYMBOLS, ABBREVIATIONS, AND ACRONYMS

AFRL	Air Force Research Laboratory
CPCM	conductor-like polarized continuum model
DFT	density functional theory
DME	dimethoxyethane
DNB	1,5-dinitrobiuret
GIL	generalized ionic liquid
He	helium
IL	ionic liquid
MMH	monomethylhydrazine
MNB	Mononitrobiuret
MP	melting point
NTO	nitrogen tetroxide
RTIL	room temperature ionic liquid
SEM	scanning electron microscope
XPS	x-ray photoelectron spectrum

**LRIR #: 14RQ11COR**

**Title: IONIC LIQUID FUELS FOR CHEMICAL PROPULSION**

**Reporting Period: Final 01 October 2013 – 30 September 2016**

**Laboratory Program Manager and**

**Laboratory Principal Investigator: Dr. S. Schneider**

**Commercial Phone: (661) 275 5759, DSN: 525 5759**

**FAX: (661) 275 5471**

**Mailing Address: 10 E. Saturn Blvd, Bldg 8451  
Edwards AFB, CA 93524-7680**

**E-Mail Address: stefan.schneider@us.af.mil**

**AFOSR Program Manager: Dr. Michael Berman**



## **1.0 INTRODUCTION**

### **1.1. TASK I**

The ionic liquid (IL) program at the Air Force Research Laboratory is investigating tailored energy-dense liquids to provide a scientific foundation for the advancement of the performance and operability envelopes of current propulsion systems. General efforts involve the discovery of energetic ILs based on heterocyclic and open-chain cations in combination with reactive anions. A major goal has been the development of IL fuels which undergo hypergolic ignition upon contact with common propulsion oxidizers. In state-of-the-art bipropellant systems,  $N_2H_4$  is the fuel and  $N_2O_4$  is the oxidizer. Both compounds are highly toxic, hydrazine being a suspected carcinogen. Replacing hydrazine with an ionic liquid which generally possesses very low volatility, and therefore virtually no vapor toxicity, would be extremely desirable if not already critical. At the same time, the toxic oxidizer should be exchanged for a high-performing, environmentally benign oxidizer like, perhaps, hydrogen peroxide (decomposition of hydrogen peroxide affords only oxygen and water), if other desired properties, especially hypergolic reactivity with the fuel, can be retained. So far, most researchers seeking hypergolic fuels have limited themselves to the extremely toxic and corrosive nitric acid solutions. While important questions remain unanswered, we are exploring new ground. During our previous work we demonstrated the hypergolicity of ILs with one class of hydrogen-rich anions toward a variety of common propellant oxidizers, including hydrogen peroxide. However, for practical purposes the materials had several shortcomings, especially poor liquid range and viscosity. Furthermore, their high hydrocarbon content limits propellant performance. Based on multiple molecular design strategies the proposed research effort focuses on synthesizing novel energetic ILs, supported by experimental mechanistic studies and computational investigations. Expanding on our previous work we intend to enlarge the chemical landscape of known light metal hydride ILs. We envision the successful completion of this project will result in:

- Fundamental understanding of the coordination of light metals in highly reducing environments.
- Expansion of the range of materials available for hydrogen storage.
- Novel solvent systems enabling unique reduction reactions.

### **1.2 TASK II**

The Ionic Liquids Ignition program investigates the chemical kinetics and reaction dynamics involved in the hypergolic and catalytic ignition of ionic liquid propellants with the purpose of identifying key intermediates and kinetic bottlenecks which can enhance or restrict performance in ionic liquid-based propulsion systems. In better understanding the energy landscape involved in hypergolic ignition of ionic liquids with various oxidizers, we can use this knowledge to support the synthetic efforts in Task I to discover viable candidate ionic liquid fuels for propulsion systems. An important goal of our research is to use sensitive and selective experimental probes to understand in real time and at the molecular level the underlying chemistry involved under relevant extreme

environments. The experimental data will provide the necessary mechanistic and chemical kinetics information, and with ab initio quantum chemical analysis, accurate reaction mechanisms will be elucidated. The combined information will feed into chemical kinetics models, which will make reactivity predictions possible for hypergolic fuels and high-temperature catalysts, leading to improved design of energetic ILs including more reliable ignition and sustained combustion.

## 2.0 TECHNICAL SUMMARY

### 2.1 TASK I

Propulsion performance can be fostered by light metals which have large combustion energies and relatively light products. Elements with considerable performance advantages and non-toxic products are aluminum and boron. In addition, high hydrogen content fulfills the need for light combustion products through the production of hydrogen gas and water vapor. ILs containing  $\text{Al}(\text{BH}_4)_4^-$  anions may be viewed as a densified form of hydrogen stabilized by metal atoms. The volumetric hydrogen content of tetraethylammonium- $\text{Al}(\text{BH}_4)_4$  is, in fact, 99% higher than that of liquid hydrogen.<sup>1</sup> Previously we reported an IL containing the  $[\text{Al}(\text{BH}_4)_4]^-$  anion but the material has several shortcomings which make it impractical to use as a propellant. In an attempt to lower the viscosity, neutral ABH was mixed with an IL containing the cyanoborohydride anion. ILs with the  $[\text{NCBH}_3]^-$  anion by itself generally possess very low viscosities ( $\sim 20\text{cp}$ ). It was anticipated that the combination of  $[\text{NCBH}_3]^-$  with ABH would produce a new anion of the formula  $[\text{Al}(\text{BH}_4)_3\text{NCBH}_3]^-$ . A couple of possibilities were considered for the binding/coordination of the  $[\text{NCBH}_3]^-$  anion to ABH. Boron and aluminum can compete for the carbon and nitrogen and calculations revealed that boron prefers carbon by  $\sim 13\text{kcal/mol}$ . Direct coordination of the CN group to aluminum is also preferred over 3-centered-2-electron hydrogen bonds by  $\sim 21\text{kcal/mol}$  (Figure 1).

However, during our previous studies we discovered that the reaction chemistry of ABH is far more complex than initially anticipated and our initial findings prompted us to investigate this chemistry in more detail.

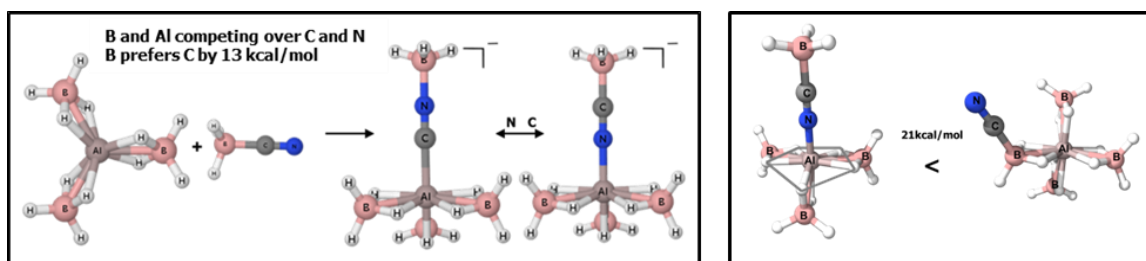


**Figure 1.** Different coordination possibilities of  $[\text{NCBH}_3]^-$  to ABH.

We established the existence of a prevalent mixed borohydride/cyanoborohydride aluminum compound with a coordination number of seven (Figure 2) and saw spectroscopic evidence that other species are present.

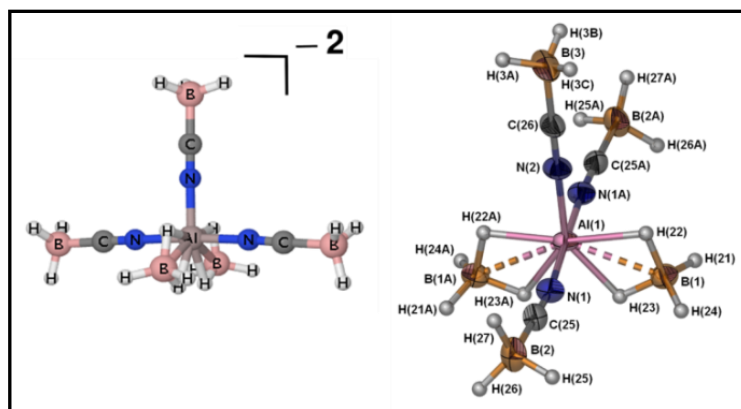
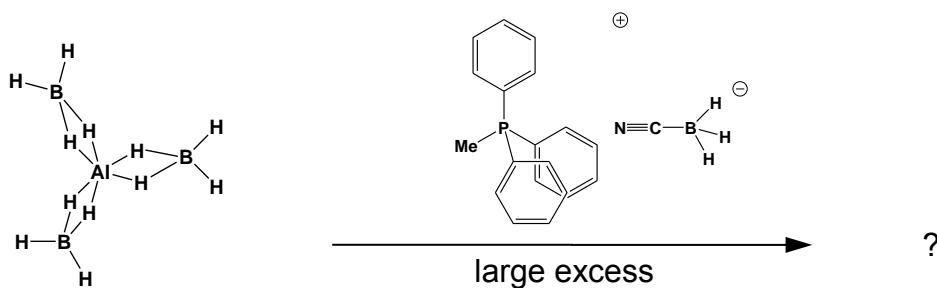


**Figure 2.** A new, doubly charged anion (calc., left; crystal structure, right)  $[Al(BH_4)_2(NCBH_3)_3]^{2-}$

In a next step we first explored the synthetic accessibility of new anions of aluminum by reacting ABH with a large amount of  $[NCBH_3]^-$ .



**Scheme 1.** Reaction of ABH with Methyl-triphenyl-phosphonium CBH.

Final composition of the only isolated product was resolved by a single crystal X-ray structure determination and the structure of the novel  $[Al(CNBH_3)_6]^{3-}$  anion is shown in Figure 3.

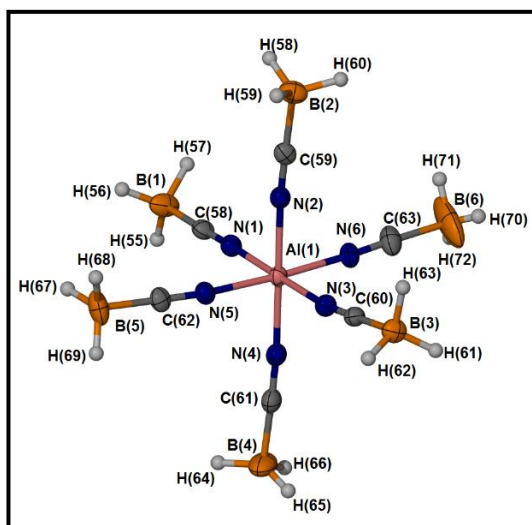
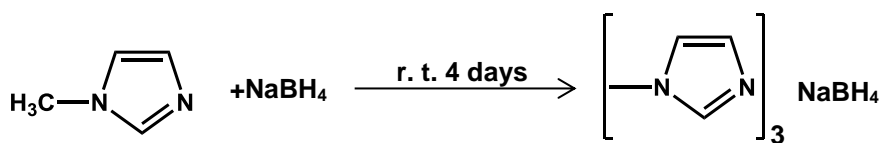


**Figure 3.** X-ray crystal structure of isolated product showing a rare example of a hexacoordinated, triply charged aluminum anion.

In 2012 the group of Ingo Krossing investigated literature known procedures to make heterocyclic borohydride salts<sup>2</sup> in great detail and determined that the best material obtainable thereby still had a halide content of at least 22.5%.<sup>3</sup> In addition they discovered a new method for preparing analytically pure borohydride salts in a mixed solvent system, liquid ammonia/methylene chloride, at low temperatures.

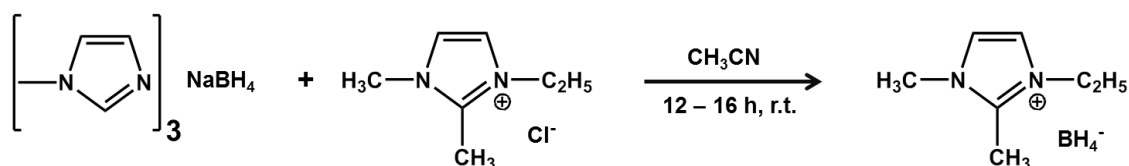
We now discovered another method which allows us to run the metathesis in a single solvent at room temperature.

We took advantage of the unique coordination possibilities of alkali metal borohydrides. The coordination complex between methylimidazole and sodium borohydride possesses a distinct characteristic which is not found in uncoordinated NaBH<sub>4</sub> (Scheme 2).



**Scheme 2.** Coordination chemistry of methylimidazole with NaBH<sub>4</sub>.

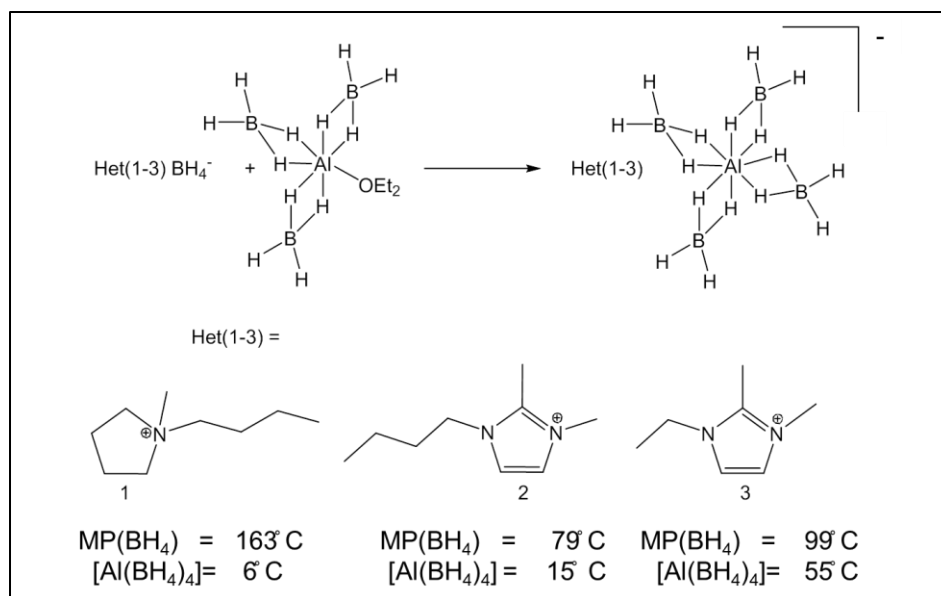
While NaBH<sub>4</sub> is soluble only up to ~2% in acetonitrile the coordination complex with methylimidazole revealed a high solubility in this solvent. Many heterocyclic halide salts are soluble in acetonitrile as well. Therefore, the new coordination complex could be used in metathesis reaction with the formation of sodium chloride and the free amine (Scheme 3). The free amine could be easily removed by washing the product with diethylether.



**Scheme 3.** Metathesis reaction between heterocyclic halide salt and NaBH<sub>4</sub> coordination complex.

Our new method has multiple advantages over the procedure developed by Krossing. Krossing has to rely on a co-solvent system, between ammonia and methylene chloride. Reactions have to be carried out at low temperature. Methylene chloride has more handling restrictions and health issues than acetonitrile. This new synthetic route to analytically pure heterocyclic borohydride salts provides the necessary starting materials for an easy conversion to a new class of ILs with complexed [Al(BH<sub>4</sub>)<sub>4</sub>]<sup>-</sup> anion.

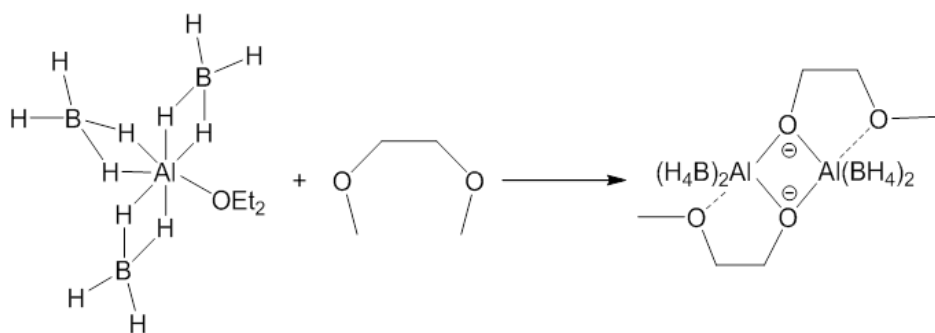
Though the melting points (MP's) of the borohydride derivatives were high (Scheme 4) it was anticipated that the liquefying nature of the aluminum borohydride anion should allow for a significant MP depression. Upon complexation two of the three salts formed viscous room temperature ionic liquids (RTIL's) (Scheme 4, compound 1 and 2), while 3 with only a 44°C MP depression was not a RTIL.



**Scheme 4.** Synthetic scheme for RTIL tetrakis-tetrahydroborate aluminate molecules

1-ethyl-2,3-dimethylimidazolum tetrakis-tetrahydroborate aluminate (3) was dissolved in a minimal amount of dimethoxyethane (DME) to carry out drop-test experiments. While the initial tests were successful a precipitate was formed after a couple days. The precipitate consisted of a new complex in which two borohydride ligands were displaced and instead a bidentate- $\mu_2$ -bridging methoxyethoxide ligand system was installed. This is the first known example of such a mixed ligand system (Scheme 5).

In order to establish that this unusual coordination is general for aluminum borohydride containing materials, the etherate of aluminum borohydride was reacted with DME (Scheme 5). The material recovered from this reaction proved to be identical to that from the previous salt solution. This demonstrates that aluminum borohydride containing compounds are not compatible with strongly coordinating solvents like DME. This will have to be considered for future development of salt/solvent systems which could deliver useful, high-hydrogen materials.



**Scheme 5.** Reaction between Aluminum borohydride-etherate and DME.

## Computational

Preliminary simulations have uncovered some of the rich chemistry inherent in the aluminum borohydrides. Oxidation by water of either the simple borohydride anion or the neutral borane molecule in the gas phase produces hydrogen gas with the formation of a boron-oxygen bond and takes place via the transition states displayed in Figure 4.

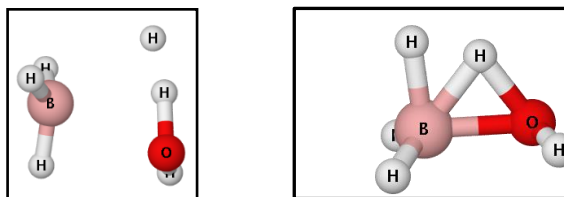


**Figure 4.** Transition states of  $\text{BH}_4^- \cdot \text{H}_2\text{O}$  and  $\text{BH}_3 \cdot \text{H}_2\text{O}$ .

It appears that oxidation of the aluminum borohydride anion,  $[\text{Al}(\text{BH}_4)_4]^-$ , does not occur directly in an analogous manner. Rather, a two-step reaction in which water initially displaces a neutral borane molecule (Figure 5, left) and subsequently reacts with it in a complex with the remaining anion (Figure 5, right) is observed in the calculation.

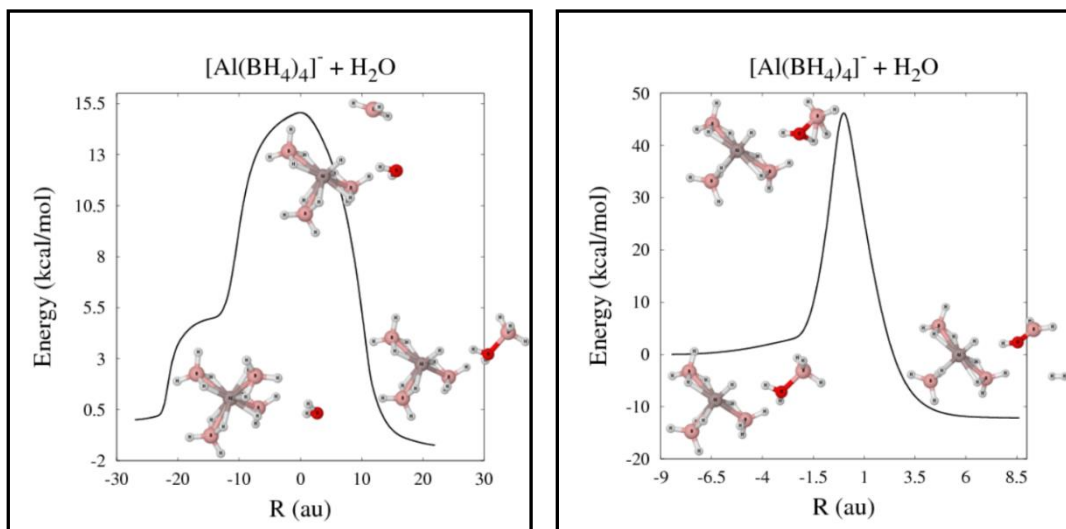


**Figure 5.** Energy profiles along the Intrinsic Reaction Coordinate (IRC) for the hydrolysis of the  $[\text{Al}(\text{BH}_4)_4]^-$ .

Additional insight into the relative reactivities of these species is gained from the calculated activation barriers and reaction energies given in Table 1. Although hydrolysis of  $[\text{Al}(\text{BH}_4)_4]^-$  nominally involves oxidation of  $\text{BH}_3$ , the presence of the intermediate anionic fragment leads to an activation barrier and reaction energy in between those for bare neutral  $\text{BH}_3$  and the bare  $[\text{BH}_4]^-$  anion. These values agree with the facts that neutral boranes are pyrophoric in moist air, that many aqueous borohydride solutions have substantial stability, and that aluminum borohydride ILs manifest considerable hydrolytic stability, perhaps intermediate between the two. Theory will help the experimental effort by predicting early intermediates such as  $[\text{H-Al}(\text{BH}_4)_3]^-$ , and modeling their vibrational spectra as an aid to identifying the species evolving in cryogenic matrices.

**Table 1.** Energies (kcal/mol) for the reactions which form H<sub>2</sub> by hydrolysis.

	Activation energy E <sub>a</sub>	Reaction energy ΔE
BH <sub>3</sub>	39	-21
[H-Al-(BH <sub>4</sub> ) <sub>3</sub> ] <sup>-</sup> + BH <sub>3</sub>	46	-12
[BH <sub>4</sub> ] <sup>-</sup>	69	+4

### TASK I Specific research goals and objectives for FY16.

Unfortunately, neither the cyanoborohydride approach nor the pure tetrakis-tetrahydroborate aluminate ILs discovered possess the desirable physical properties for a suitable propellant. In general, their major shortcomings still are poor liquid range and high viscosity as well as the high hydrocarbon content of the cations required to lower their melting points which severely limits propellant performance.

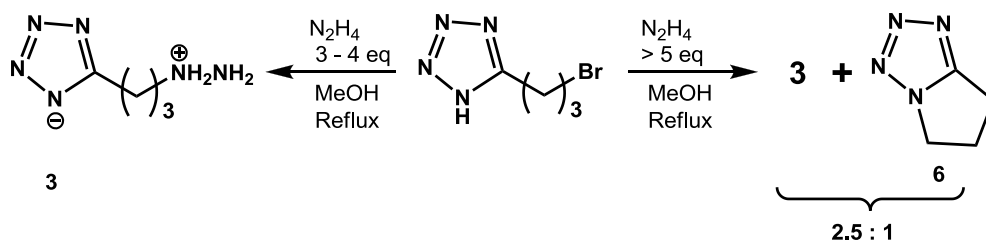
In light of our discoveries we turned to systems simpler and higher performing than the complexed Al(BH<sub>4</sub>)<sub>4</sub><sup>-</sup> anions. Solutions of Li-Al hydrides and LiBH<sub>4</sub> in ethers have shown some desirable propellant properties,<sup>4</sup> and a variety of lithium metal hydrides are commercially available. This suggested an entry point into the coordination chemistry of lithium salts with some new high energy heterocyclic ring systems. Our studies on some of these promising new heterocyclic systems is summarized below, however, the objective for this last performance period were:

1. Study stable lithium borohydride tetrazole complexes.
2. Study lithium borohydride complexes of simple amines with high borohydride-to-amine ratios.

### Synthesis of 5-substituted tetrazoles as novel ligands and energetic salts

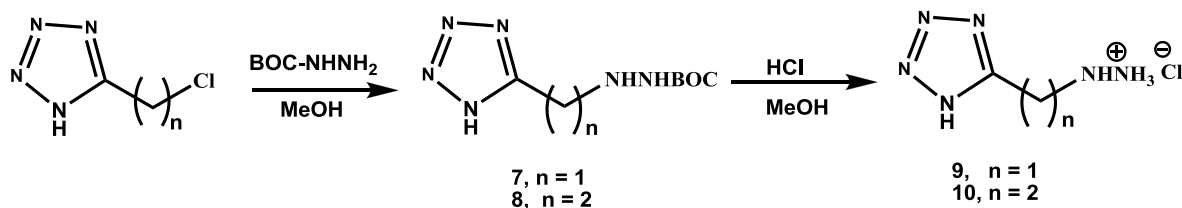
In pursuit of functionalized energetic heterocycles suitable to form stable coordination compounds with metal borohydrides, the highly energetic tetrazole ring system was chosen and it was desired to incorporate different hydrazine moieties. Hydrazines are still the *State of the Art* propellants and it was hoped to retain some of their desirable properties in a new hydrazinotetrazole derivative.

At first it was envisioned that simple nucleophilic substitutions would be a straight forward approach to prepare 5-(hydrazino-alkyl) tetrazoles (Scheme 6).



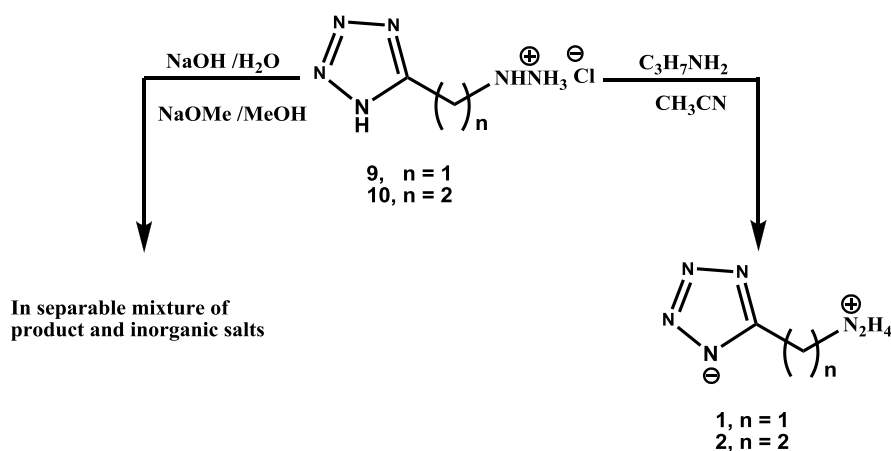
**Scheme 6.** Synthesis of 5-(hydrazino-propyl) 1H tetrazole **3** and trimethylene tetrazole **6**.

Disappointingly our initial approach of a single step replacement of the halide group with a hydrazine moiety leading to pure 5-(hydrazino-alkyl)-1H-tetrazoles **1** and **2** were not successful. Thus an alternative multistep synthetic route involving the use of BOC protected hydrazine as a substrate was devised (Scheme 7).



**Scheme 7.** Synthesis of hydrochloride salts **9** and **10**

Initial attempts to neutralize the hydrochloride salt **9** with standard alkaline bases as well as metal alkoxides led to inseparable mixtures of inorganic salt and the desired 5-(hydrazino-methyl) tetrazole **1**. A lengthy washing and filtering procedure was employed which finally afforded 5-(hydrazino-methyl)-1-H-tetrazoles **1** as clean white powder (Scheme 8). X-ray quality crystals of **1** were obtained by diffusion of diethyl ether into methanol solution (Figure 6).



**Scheme 8.** Synthesis of 5-(hydrazino-methyl), 5-(hydrazino-ethyl) tetrazoles **1** and **2**

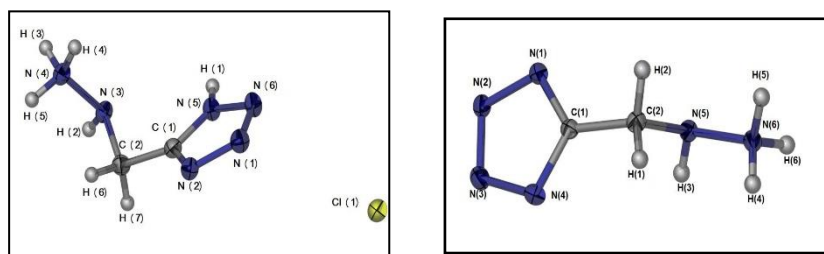


**Figure 6.** Single crystal X-ray structure of the hydrochloride **9** and 5-(hydrazino-alkyl) tetrazoles **1**.



The coordination chemistry of lithium borohydride has been studied previously. Almost 70 years ago its coordination with ammonia<sup>5</sup> was investigated and more recently much work was carried out emphasizing the structural chemistry of lithium borohydride with various types of coordinating ligands.<sup>6-9</sup> Most notably Nöth et. al. have developed a methodology for describing the interaction of the hydrogens with the metal center in coordination compounds. His work demonstrated the very complicated relationship between the borohydride and the metal, influenced by the electronic and steric demands of the ligands (Figure 7).<sup>6</sup>

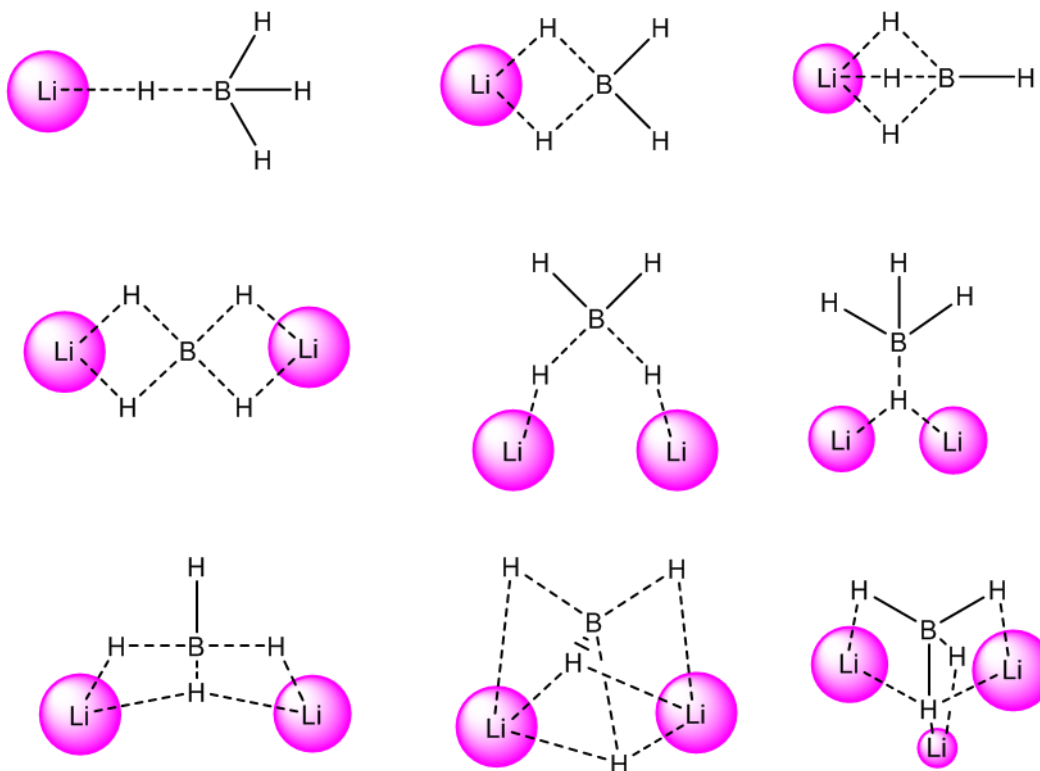
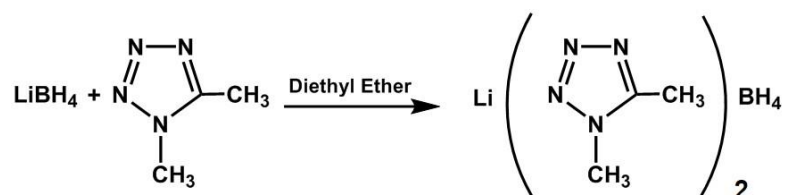


**Figure 7.** Modes of borohydride coordination with metal centers in solvated systems

Our preliminary ventures into the coordination chemistry of lithium borohydride have concentrated on the coordination of high nitrogen ligands. Over the last decade high nitrogen compounds have become fundamental to the search for new energetic materials.

1,5-dimethyltetrazole forms a complex with a 1:2 lithium to ligand ratio (Scheme 9). It is interesting to note that the ligand bridge the two lithium metal centers (Figure 8). This is the first example where two different nitrogen atoms of the same ring coordinate and bridge multiple lithium cations.



**Scheme 9.** Coordination of 1,5-dimethyltetrazole with lithium borohydride

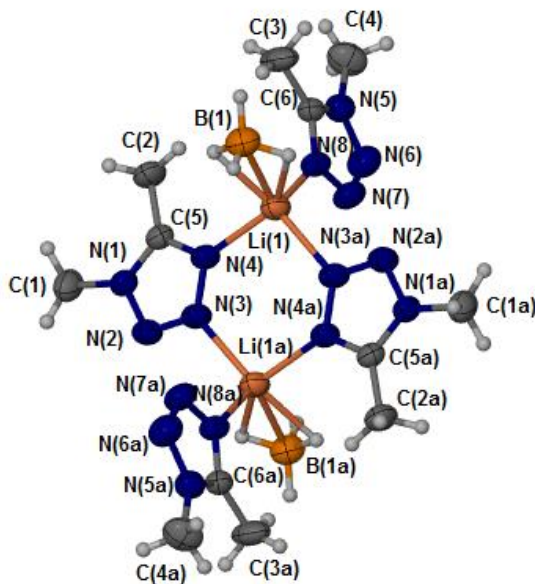
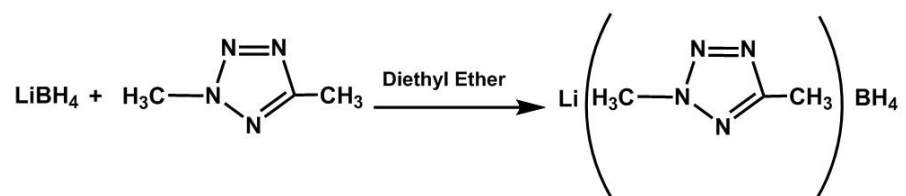


**Figure 8.** Crystal Structure of  $\text{Li} (1,5\text{-dimethyltetrazole})_2 \text{BH}_4$

Interestingly, a modest change in the steric interactions by isomerization to the 2,5-dimethyltetrazole derivative resulted in a 1:1 complex (lithium to ligand) (Scheme 10).



**Scheme 10.** Coordination of 2,5-dimethyltetrazole with lithium borohydride

The resulting polymeric structure shows extended lithium and borohydride interactions. To our knowledge this is the first example of this type of bonding motif with lithium borohydride (Figure 9).

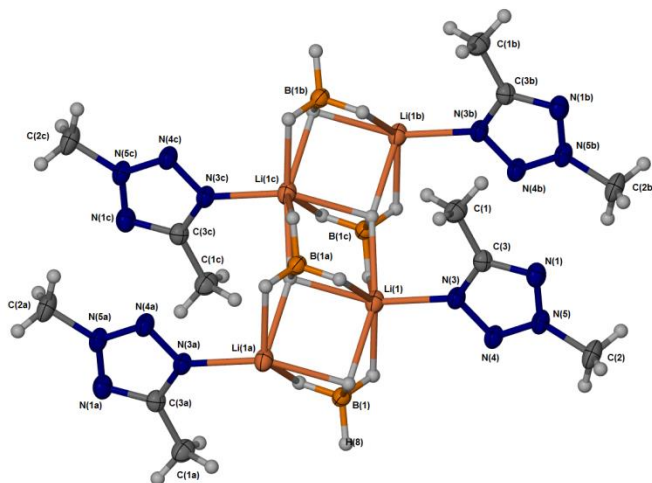


**Figure 9.** Crystal structure of  $\text{Li}(2,5\text{-Dimethyltetrazole})\text{BH}_4$

In the context of the work by Nöth et. al., the two different coordination complexes confirm the very diverse role that the borohydride ligand plays. More important from a propellants perspective is the change in stoichiometry of the performance enhancing borohydride with such a small change in structure. Although both complexes are solids at ambient temperature, our overall goal is to solvate  $\text{LiBH}_4$  at a high mole ratio and the general presence of multiple bonding modes might aid in liquefying these systems. As a next step coordination with the low boiling amine, methylamine, was investigated. A 2:3 lithium to amine ratio was determined by  $^1\text{H}$  NMR (Figure 10). No undesirable amino borane side product was observed as can be seen by the single pentet present in the  $^{11}\text{B}$  NMR (Figure 11).

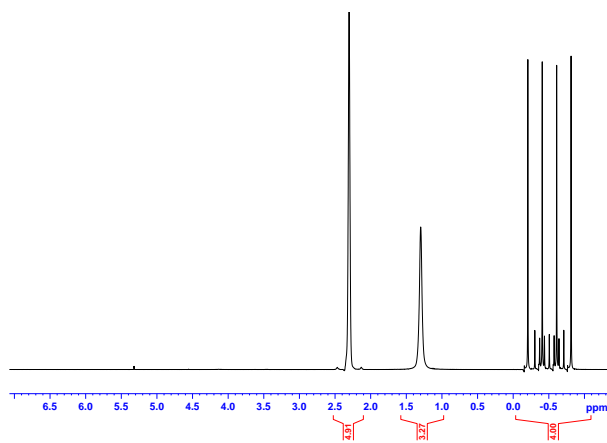


**Figure 10.**  $^1\text{H}$  NMR of  $\text{Li}_2(\text{H}_2\text{NCH}_3)_3(\text{BH}_4)_2$

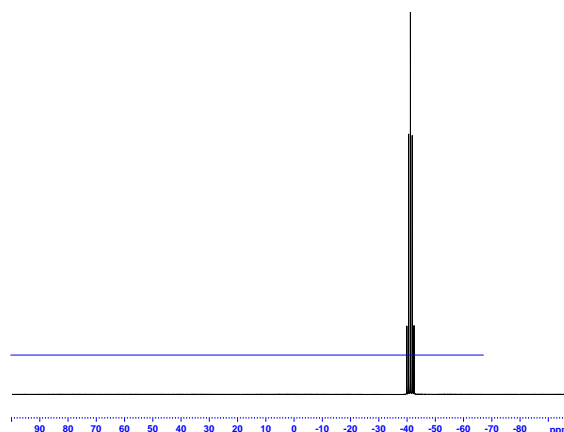


**Figure 11.**  $^{11}\text{B}$  NMR of  $\text{Li}_2(\text{H}_2\text{NCH}_3)_3(\text{BH}_4)_2$

Surprisingly, this complex showed a melting point of only 4°C and appeared to be thermally stable with no decomposition visible until ~180°C according to DSC data (Figure 12). Upon further analysis by TGA-MS, it was seen that the coordination of the amine was not as strong as initially supposed. The methylamine ligand (mass 31) is almost immediately lost upon heating (Figure 13). However, this represents the first example of a room temperature liquid LiBH<sub>4</sub> complex.

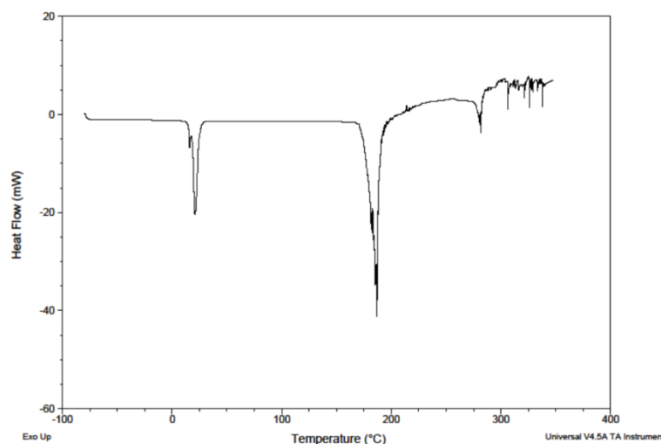


**Figure 12.** DSC of  $\text{Li}_2(\text{H}_2\text{NCH}_3)_3(\text{BH}_4)_2$

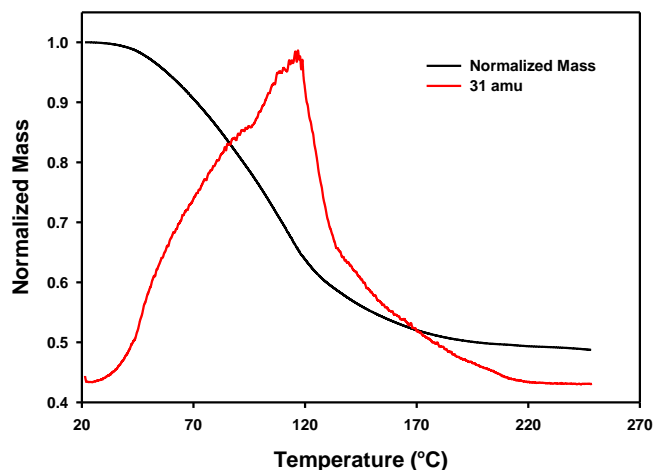


**Figure 13.** TGA-MS of  $\text{Li}_2(\text{H}_2\text{NCH}_3)_3(\text{BH}_4)_2$

At this stage in our preliminary studies we decided to investigate other ligands with chelating abilities. The first ligand investigated was diethylenetriamine as an analogue to the known Li-glyme complexes (Figure 14).



**Figure 14.** Solvation by diethylenetriamine compared to the known Li-glyme-complex.

According to NMR spectroscopy a 1:1 lithium to ligand complex was formed (Figure 15). Observations with water as the solvent for the initial NMR were tantalizing. While NaBH<sub>4</sub> solutions are known to be water stable for quite some time at a pH of 10, LiBH<sub>4</sub> has marginal hydrolytic stability.

Even though the water used for our NMR samples had a pH of 4, we were surprised to note very little gas evolution upon dissolving the complex and the immediately recorded  $^1\text{H}$  and  $^{11}\text{B}$  NMR spectra showed only very slight hydrolysis. Further spectra taken after 2 days and 5 days showed only minimal hydrolysis of the  $\text{LiBH}_4$  complex (Figure 16). We believe this is the first time a water stable complex of  $\text{LiBH}_4$  has been observed (at least short term) and that these complexes should certainly be investigated for their ability to be practical reducing agents in water solutions.

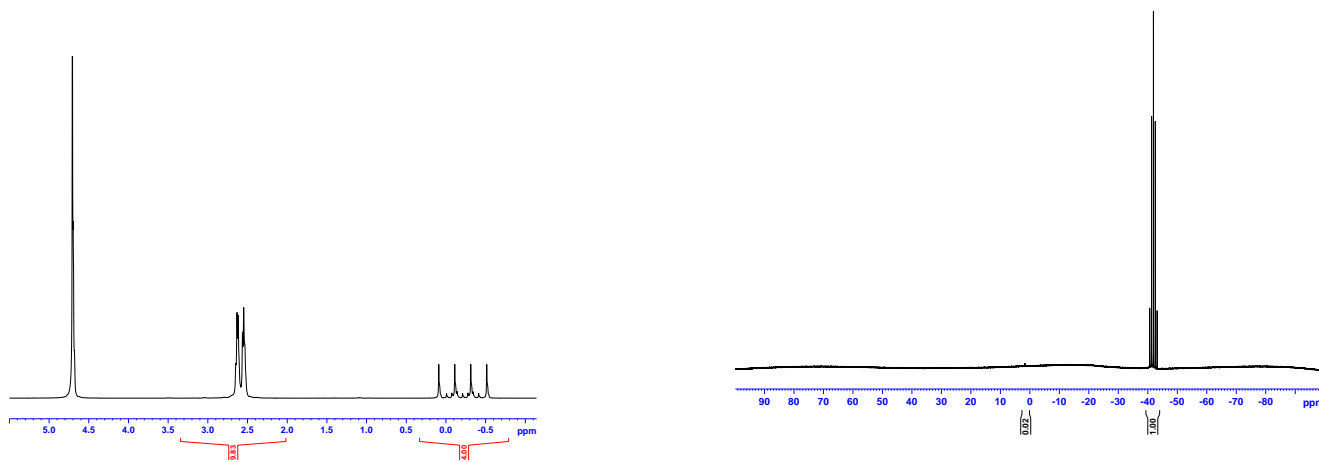


**Figure 15.** Initial  $^1\text{H}$  (left) and  $^{11}\text{B}$  NMR (right) of  $\text{Li}(\text{diethylenetriamine})\text{BH}_4$

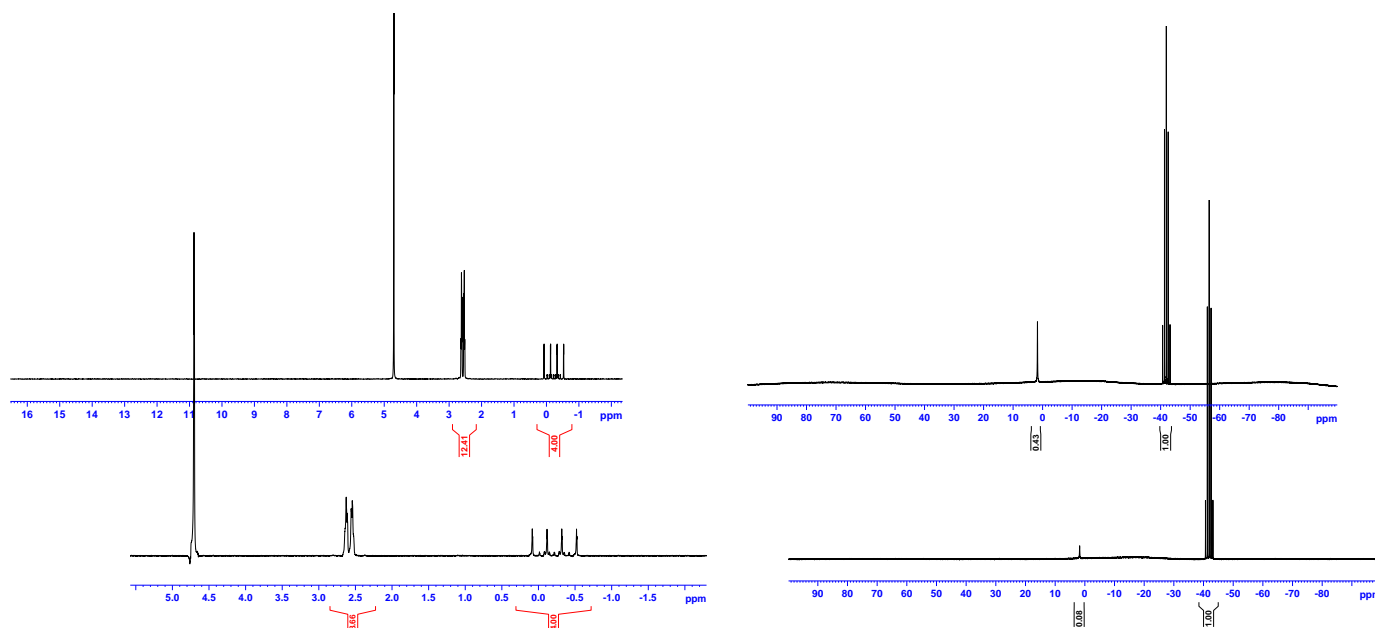


**Figure 16.**  $^1\text{H}$  (left) and  $^{11}\text{B}$  NMR (right) of  $\text{Li}(\text{diethylenetriamine})\text{BH}_4$  after 2d (bottom), after 5d (top)

## Collaborations

An important collaboration was established with Purdue University (Prof. Timothée Pourpoint). Under an AFRL-funded SBIR contract a small thrust stand was developed by Orbitec (Orbital Technologies Corporation) and delivered to Purdue University. This government-furnished equipment (Figure 17) was modified during a 2015 effort funded by our laboratory to allow it to accommodate our new fuels and complementary oxidizers. This test stand will be used to learn more about the combustion characteristics of molecular fuels containing light metals and will therefore quantify how much of the promised performance is likely to be possible. This constitutes an essential step in guiding the transition from research synthesis to propellant development. The miniature test-bed thruster will be operated at about 1 to 5 lbf with an impinging jet configuration. The purpose of this thruster is to allow for performance characterization in terms of  $C^*$  and  $I_{sp}$ . It has a flexible design that permits the use of replaceable injectors, nozzles, and combustion chambers of various sizes. Measurements include thrust, chamber pressure, and chamber temperature. Some of the preliminary 2015 test results are depicted below showing a drop test result (Figure 18) and successful test firing of a boron containing fuel developed during our efforts (Figure 19 left). The research effort will include optimizing system parameters as well as oxidizer to fuel ratios to demonstrate acceptable combustion efficiencies not realized during our initial tests (Figure 19 right).



**Figure 17.** Modified test stand installed at Purdue University, Zucrow Test Facility

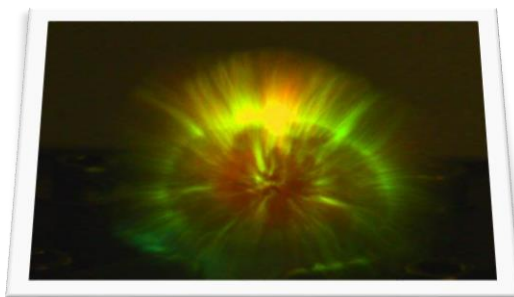


**Figure 18.** Drop test image of AFRL fuel and WFNA: Ignition within 1.1ms

Distribution A: Approved for Public Release; Distribution unlimited

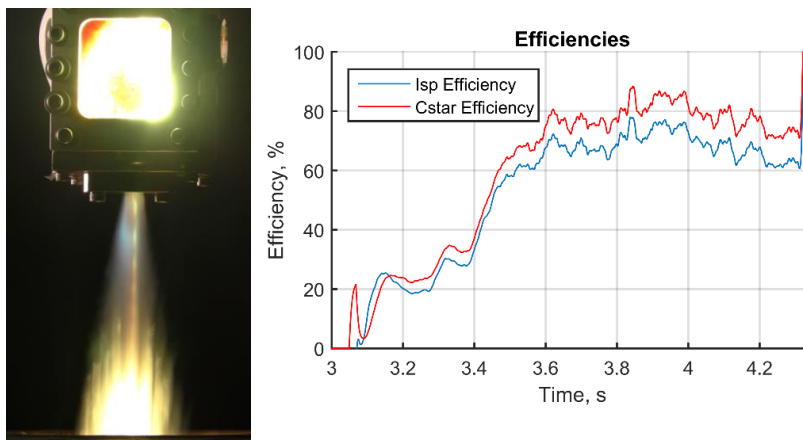


**Figure 19.** Successful hotfire-test at Purdue University measured ISP and C\* efficiency

### References Task I

- 1 Schneider, S.; Hawkins, T.; Ahmed, Y.; Rosander, M.; Hudgens, L.; Mills, J. *Angew. Chem. Int. Ed.* **2011**, 50, 5886-5888.
- 2 a) Wang, J.; Song, G.; Peng, Y.; Zhu, Y. *Tetrahedron Lett.* **2008**, 49, 6518-6520; b) Zhang, Y.; Shreeve, J.M. *Angew. Chem. Int. Ed.* **2011**, 50, 935-937.
- 3 Bürchner, M.; Erle, A.M.T.; Scherer, H.; Krossing, I. *Chem. Eur. J.* **2012**, 18, 2254-2262.
- 4 a) J. J. Rusek, Proceedings of the 2nd International Conference on Green Propellants for Space Propulsion (ESA SP-557), Sardinia, Italy June 2004; b) T. L. Pourpoint, J. J. Rusek, 5<sup>th</sup> International Hydrogen Peroxide Propulsion Conference, Purdue University, West Lafayette, IN, September 2002.
- 5 Sullivan, E.A.; Johnson, S. *J. Phys. Chem.*, **1959**, 63(2), pp 233–238.
- 6 Giese, H.-H; Nöth, H.; Schwenk, H.; Thomas, S. *Eur. J. Inorg. Chem.*, **1998**, 941-949.
- 7 Ruiz, J.C.G.; Nöth, H.; Warchhold, M. *Eur. J. Inorg. Chem.*, **2008**, 251-266.
- 8 Aguilar-Martínez, M.; Félix-Baéz, G.; Pérez-Martínez, C.; Nöth, H.; Flores-Parra, A.; Colorado, R.; Galvez-Ruiz, J.C. *Eur. J. Inorg. Chem.*, **2010**, 1973-1982.
- 9 Leiner, S.; Mayer, P.; Nöth, H. *Z. Naturforsch.* **2009**, 64b, 793-799.

## 2.2 TASK II

The theoretical performance of RTILs can be superior to the currently used fuels for both bipropellant and monopropellant applications. Implementation by the Air Force of such RTILs would be in accordance with the green propellant initiative and would meet the emerging demands of the DoD. While RTILs show promise as enabling energetic propellants, very little is understood about the fundamental reaction chemistry involved in the energy release processes that ensue upon decomposition/oxidation of these fuels. Achieving reliable ignition and sustained combustion in RTILs are important challenges for the Air Force.

In this effort, we have carried out complementary experimental and theoretical studies on a select few model RTILs and related compounds to gain fundamental insight into the reaction chemistry of these substances. Below, we provide a summary of our findings. Detailed descriptions of the work performed and the conclusions reached may be found in articles published during the tenure of this research.

### **TASK II Research goals and objectives FY14-FY16.**

In order to model the ignition behavior of energy dense materials, such as room-temperature ionic liquids (RTILs), an important goal for this research effort was to improve the understanding of the reactive intermediate chemistry involved. The following objectives were pursued towards this end:

1. Elucidate the nature of the reaction mechanism involved in the thermolysis of model RTILs.
2. Elucidate the nature of the reaction mechanism involved in the oxidation of DCA-based RTILs.
3. Investigate reaction kinetics and flammability envelopes of hypersonic mixtures.

### **Thermal decomposition of CN ionic liquids.<sup>10</sup>**

The thermal decomposition of alkylimidazolium ionic liquids with cyano-functionalized anions has been investigated by multiple, complementary experimental techniques and density functional theory (DFT) conductor-like polarized continuum model (CPCM)-generalized ionic liquid (GIL) calculations. Due to the unusually high heats of vaporization of RTILs, volatilization of RTILs through thermal decomposition and vaporization of the decomposition products can be significant. Upon heating of cyano-functionalized anionic RTILs in vacuum, their gaseous products were detected experimentally via tunable vacuum ultraviolet photoionization mass spectrometry performed at the Chemical Dynamics Beamline 9.0.2 at the Advanced Light Source. Experimental evidence for di- and tri-alkylimidazolium cations and cyano-functionalized anionic RTILs confirms thermal decomposition occurs primarily through two pathways: (1) deprotonation of the cation by the anion and (2) dealkylation of the imidazolium cation by the anion (Figure 20). Secondary reactions include possible cyclization of the cation and C2-substitution on the imidazolium, and their proposed reaction mechanisms are discussed in detail in Ref 10. Two common thermal decomposition mechanisms have been confirmed, carbene formation and alkyl abstraction, which are related to anion basicity and nucleophilicity, respectively. Here we propose a third mechanism that likely proceeds through the carbene, which allows for addition



of S or –NCN groups to the C2 position on the imidazole ring and could be useful for synthesis of substituted C2-imidazoles. Additional evidence supporting these mechanisms was obtained using thermal gravimetric analysis/mass spectrometry, gas chromatography/mass spectrometry and temperature-jump infrared spectroscopy.

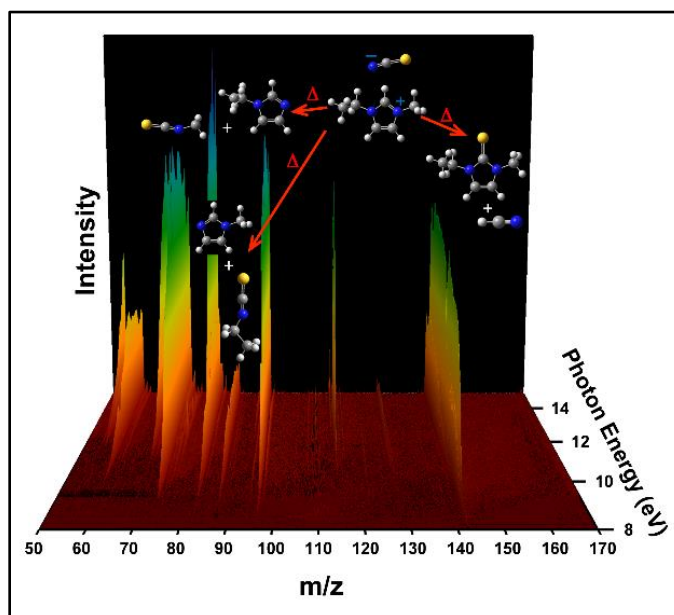


**Figure 20.** Thermal decomposition mechanisms of EMIM<sup>+</sup>SCN<sup>-</sup>, including –CH<sub>3</sub> and –CH<sub>2</sub>CH<sub>3</sub> abstractions and S substitution at EMIM C2 evidenced by vacuum ultraviolet-time of flight mass spectrometry.

In order to predict the overall thermal stability in these ionic liquids, the ability to accurately calculate both the basicity of the anions and their nucleophilicity in the ionic liquid is critical. Both gas-phase and condensed-phase (CPCM-GIL) density functional theory calculations support the decomposition mechanisms and, the CPCM-GIL model could provide an accurate means to determine thermal stabilities for ionic liquids in general. M06 density functional calculations in the gas phase and the SMD (continuum solvation model)-GIL variant of the CPCM for the condensed phase have demonstrated the ability to predict trends in anion basicity and anion nucleophilicity in pure ionic liquids, which should prove useful in predicting thermal stability trends in dialkylimidazolium ionic liquids and could be used as a higher accuracy method than the gas-phase DFT approach for predicting thermal stabilities of ionic liquids in general. One important finding from the comparison of the gas-phase basicities relative to the GIL condensed-phase basicities is that DCA<sup>-</sup> is more basic than NO<sub>3</sub><sup>-</sup> in the condensed phase ionic liquid, which indicates that the proton transfer from HNO<sub>3</sub> to DCA<sup>-</sup> is likely the first step in the hypergolic ignition mechanism (Table 2).

**Table 2.** Calculated free energies of acidity,  $\Delta G_{\text{acid}}$ , in the gas phase and in the condensed phase by SMD-GIL and SMD (water) at the M06/6-31+G(d,p) level of theory. Note that while HDCA (HNCNCN) is more acidic than  $\text{HNO}_3$  in the gas phase, in the SMD-GIL condensed-phase,  $\text{HNO}_3$  is more acidic than HDCA, possibly facilitating proton transfer from  $\text{HNO}_3$  to  $\text{DCA}^-$ :  $\text{HNO}_3 + \text{DCA}^- \rightarrow \text{NO}_3^- + \text{HDCA}$ .

acid	$\Delta G_{\text{acid}}(\text{g})$ (kJ/mol)		$\Delta G_{\text{acid}}(\text{l})$ SMD-GIL (kJ/mol)		$\Delta G_{\text{acid}}(\text{l})$ SMD- $\text{H}_2\text{O}$ (kJ/mol)
HNCS	1332.5	HNCS	607.0	HNCS	549.5
$\text{HNO}_3$	1306.7	HNCNCN	578.0	HNCNCN	521.8
HSCN	1274.2	$\text{HNO}_3$	566.6	Hvdca 04	515.2
HNCNCN	1272.6	Hvdca 01	565.2	Hvdca 01	514.6
NCNHCN	1234.6	Hvdca 04	564.9	NCNHCN	495.9
Hvdca 01	1212.1	NCNHCN	550.3	$\text{HNO}_3$	494.9
Hvdca 04	1203.3	HSCN	548.8	HSCN	492.6
HTCM (central)	1197.1	HTCM (central)	537.9	HTCM (central)	490.5
HTCM (terminal)	1188.7	HTCM (terminal)	533.9	HTCM (terminal)	483.9
Hvdca 02	1152.7	Hvdca 03	518.1	Hvdca 03	471.4
Hvdca 03	1146.1	Hvdca 02	517.6	Hvdca 02	468.6

vdca = vinylogous dicyanamide, Hvdca 01 = terminal NH, Hvdca 02 =  $-\text{CCN}_1\text{H}$ , Hvdca 03 =  $-\text{CCN}_2\text{H}$ , Hvdca 04 = central NH

### Reaction of aerosolized DCA-ILs.<sup>11</sup>

The unusually high heats of vaporization of RTILs complicate the utilization of thermal evaporation to study ionic liquid reactivity. Although effusion of RTILs into a reaction flow-tube or mass spectrometer is possible, competition between vaporization and thermal decomposition of the RTIL can greatly increase the complexity of the observed reaction products. In order to investigate the reaction kinetics of a hypergolic RTIL, 1-butyl-3-methylimidazolium dicyanamide ( $\text{BMIM}^+\text{DCA}^-$ ) was aerosolized and reacted with gaseous nitric acid, and the products were monitored via tunable vacuum ultraviolet photoionization time-of-flight mass spectrometry at the Chemical Dynamics Beamline 9.0.2 at the Advanced Light Source. Reaction product formation at  $m/z$  42, 43, 44, 67, 85, 126, and higher masses was observed as a function of  $\text{HNO}_3$  exposure. The identities of the product species were assigned to the masses on the basis of their ionization energies.

To our knowledge, this is the first study on the chemical reactivity of ionic liquid aerosols. Measurement of the product profiles as a function of  $\text{HNO}_3$  exposure allows for insight into the kinetics of the initial reaction steps in the hypergolic reaction of  $\text{BMIM}^+\text{DCA}^- + \text{HNO}_3$ . Kinetics analysis indicates that the initial reaction of  $\text{BMIM}^+\text{DCA}^-$  with  $\text{HNO}_3$  is much faster than the subsequent reaction of HDCA with  $\text{HNO}_3$ . The observed exposure profile of the  $m/z$  67 ( $\text{HDCA}^+$ ) signal suggests that the excess gaseous  $\text{HNO}_3$  initiates rapid reactions near the surface of the RTIL aerosol (Figure 21). Nonreactive molecular dynamics simulations support this observation, suggesting that diffusion within the particle may be a limiting step. The mechanism is consistent with previous reports that nitric acid forms a protonated dicyanamide species in the first step of the reaction,<sup>12</sup> and this work is the first to directly detect the formation of HDCA. Additional FTIR experimental results indicate that  $\text{NO}_2^+$  appears not to be an important species in the hypergolic ignition mechanism.

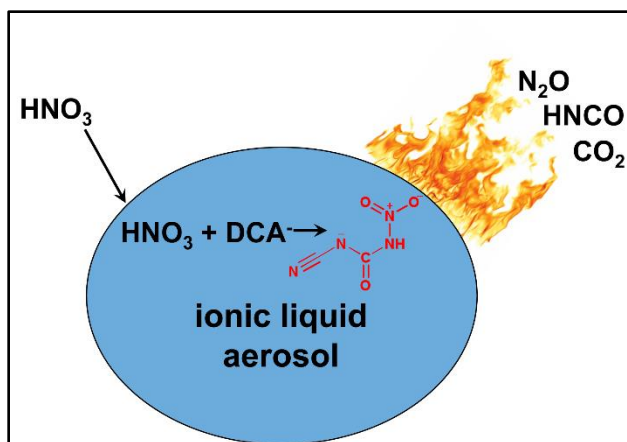


**Figure 21.** Depiction of the diffusion-limited process in the ignition of hypergolic DCA-based ionic liquids with  $\text{HNO}_3$ .

### Reactivity of B- and Al-nanoparticle infused ionic liquids.<sup>13</sup>

The interaction of H-functionalized boron nanoparticles with alkenes and nitrogen-rich ILs was investigated by a combination of X-ray photoelectron spectroscopy, FTIR spectroscopy, dynamic light scattering, thermogravimetric analysis, and helium ion microscopy. Surface B–H bonds are shown to react with terminal alkenes to produce alkyl-functionalized boron particles. The interaction of nitrogen-rich ILs with the particles appears, instead, to be dominated by boron–nitrogen bonding, even for ILs with terminal alkene functionality.

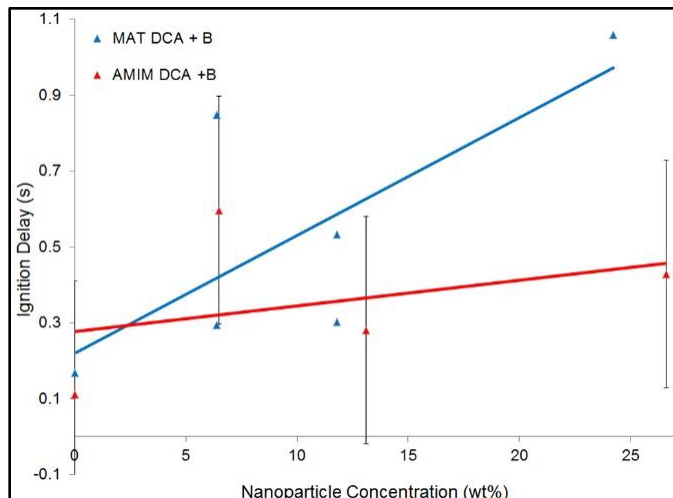


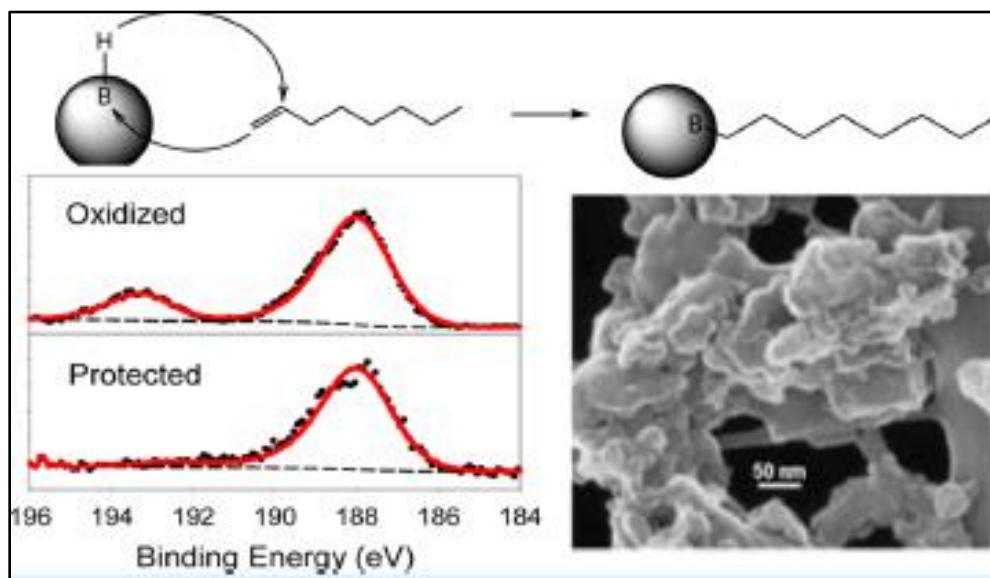
**Figure 22.** Ignition delay time of boron nanoparticle-infused ionic liquids  $\text{MAT}^+\text{DCA}^-$  and  $\text{AMIM}^+\text{DCA}^-$  as a function of particle loading as determined by the evolution of  $\text{CO}_2$  by rapid-scan Fourier-transform infrared spectroscopy.

This chemistry provides a convenient approach to producing and capping boron nanoparticles with a protective organic layer, which is shown to protect the particles from oxidation during air exposure. By controlling the capping group, particles with high dispersibility in nonpolar or polar

liquids can be produced. For the particles capped with ILs, the effect of particle loading on hypergolic ignition delay times of the ILs is reported in Figure 22.

Milling of boron in  $H_2$ , followed by mix-milling with a capping agent, is shown to be an efficient way to produce boron nanoparticles capped with either alkyl groups or ionic liquids. IR spectroscopy suggests that the alkyl capping process involves reaction of terminal C=C bonds in alkene capping agents with B-H bonds on the surface, resulting in B-C bond formation. For the ionic liquids, the mode of binding to the surface is more difficult to determine unambiguously. There is no obvious difference in the mode of binding of ILs with and without terminal C=C bonds (AMIM<sup>+</sup>DCA<sup>-</sup> and MAT<sup>+</sup>DCA<sup>-</sup>, respectively), and the strong perturbation of the C≡N stretching vibrations of the DCA<sup>-</sup> anion in the capping layer suggests that boron-DCA interaction is important in the bonding. Both IR and zeta potential measurements suggest that for MAT<sup>+</sup>DCA<sup>-</sup>-capped particles, the mode of binding is somewhat different for particles with, and without hydrogen termination.

Both alkyl- and IL-capped particles are protected against air oxidation, even if the samples are repeatedly ultrasonicated in solvents to remove any weakly complexed capping agents. Several mechanisms may contribute to the oxidation resistance. The organic capping layers may physically exclude  $O_2$  and water (the primary atmospheric oxidants) to some extent, however, given that the samples were heated overnight to 350 K, (octene boiling point = 394 K), and exposed to air for at least 6 hr prior to XPS analysis (Figure 23), it seems unlikely the capping layer could simply be functioning as a diffusion barrier. More likely, bonding of the capping layer to the surface changes the surface chemistry, such that it is unreactive to  $O_2$  and water up to 350 K.

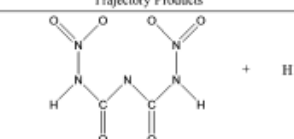
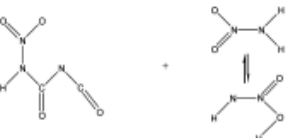
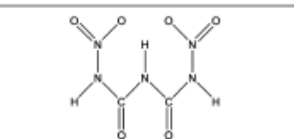
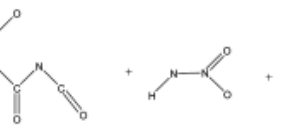
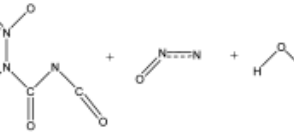
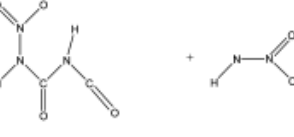


**Figure 23.** X-ray photoelectron spectrum (XPS, left) of the oxidized and protected boron nanoparticles, and scanning electron microscope image (SEM, right) of the ball milled boron nanoparticles that have been protected.

### MD calculations of thermal decomposition of DNB.<sup>14</sup>

Certain room-temperature ionic liquids exhibit hypergolic activity as liquid bipropellants. Understanding the chemical pathways and reaction mechanisms associated with hypergolic ignition is important for designing new fuels. It has been proposed<sup>12</sup> that an important ignition step for the hypergolic ionic liquid bipropellant system of dicyanamide/nitric acid is the activation and dissociation of the 1,5-dinitrobiuret anion  $\text{DNB}^-$ . For the work reported here, a quasiclassical direct dynamics simulation, at the DFT/M05-2X level of theory, was performed to model  $\text{H}^+ + \text{DNB}^-$  association and the ensuing unimolecular decomposition of HDNB. This association step is 324 kcal/mol exothermic, and the most probable collision event is for  $\text{H}^+$  to directly scatter off of  $\text{DNB}^-$ , without sufficient energy transfer to  $\text{DNB}^-$  for  $\text{H}^+$  to associate and form a highly vibrationally excited HDNB molecule. However, approximately 1/3 of the trajectories do form HDNB, which decomposes by eight different reaction paths and whose unimolecular dynamics is highly nonstatistical. Some of these paths are the same as those found in a direct dynamics simulations study of the high-temperature thermal decomposition of HDNB<sup>15</sup> for a similar total energy.

**Table 3.** Direct dynamics trajectory simulation results for  $\text{H}^\bullet + \text{DNB}^\bullet$  collisions.

Path	Trajectory Products	Trajectory Ratios(%)
1	 + H	66.7
2		26.0
3		2.7
4		1.7
5		1.0
6		1.0
	Sum of other dissociation paths <sup>a</sup>	1.0

The reaction pathways found in the direct dynamics simulation modeling of  $\text{H}^+ + \text{DNB}^-$  collisions are shown in Table 3. Possible formation of the highly vibrationally excited HDNB molecule is modeled by assuming an electronic transition from the  $\text{H}^+ + \text{DNB}^-$  to  $\text{H}\bullet + \bullet\text{DNB}$  potential energy surface and simulating the collisions on this latter surface. The most likely event, that is, 2/3 of the trajectories, is for the H-atom to directly scatter off of  $\bullet\text{DNB}$  without forming a “hot” HDNB molecule. For most of the trajectories, an insufficient amount of the  $\text{H}\bullet + \bullet\text{DNB}$  relative translational energy is transferred to  $\bullet\text{DNB}$  vibrational energy to form a vibrationally excited HDNB molecule. Another way to view these dynamics is that there is insufficient IVR (internal vibrational energy redistribution) from the incipient H–DNB bond of the  $\text{H}\bullet + \bullet\text{DNB}$  collision to other vibrational modes, and the  $\text{H}\bullet$  atom directly scatters from  $\bullet\text{DNB}$ . Approximately 1/4 of the trajectories followed path 2 in Table 3, forming the  $\text{H}_2\text{N}_2\text{O}_2$  product, which has an isomerization pathway to  $\text{HNNOOH}$ . The  $\text{H}_2\text{N}_2\text{O}_2/\text{HNNOOH}$  product pathway may undergo seven different secondary dissociations. This reaction occurs by the colliding H-atom first interacting with the central N-atom and the two adjacent O-atoms of  $\bullet\text{DNB}$ , which is then followed by IVR promoting the chemical reaction. This was found to also be an important pathway for HDNB dissociation in a previous direct dynamics simulation by Liu et al.,<sup>10b</sup> for which HDNB was thermally excited. In summary, a comparison of the current results with the previous study by Liu et al.<sup>10b</sup> shows that the initial conditions for the excited HDNB moiety are crucial for its ensuing unimolecular dynamics.  $\text{H}^+ + \text{DNB}^-$  association localizes the energy in HDNB, creating a “hot spot”, and IVR is not sufficiently rapid to result in the unimolecular dynamics found by Liu et al. for their random, thermal initial conditions. For this previous simulation, there were rapid statistical interconversions between all of the HDNB conformers before unimolecular dissociation occurred. In future work, it would be of interest to study both the random and nonrandom excitation of HDNB in a condensed phase liquid environment.

#### High-level *ab initio* calculations of DNB.<sup>16</sup>

Mononitrobiuret (MNB) and 1,5-dinitrobiuret (DNB) are tetrazole-free, nitrogen-rich, energetic compounds. For the first time, a comprehensive *ab initio* kinetics study on the thermal decomposition mechanisms of MNB and DNB has been carried out. In particular, the intramolecular interactions of amine H-atom with electronegative nitro O-atom and carbonyl O-atom have been analyzed for biuret, MNB, and DNB at the M06-2X/aug-cc-pVTZ level of theory. The results show that the MNB and DNB molecules are stabilized through six-member-ring moieties via intramolecular H-bonding with interatomic distances between 1.8 and 2.0 Å, due to electrostatic as well as polarization and dispersion interactions. Furthermore, it was found that the stable molecules in the solid state have the smallest dipole moment amongst all the conformers in the nitrobiuret series of compounds, thus revealing a simple way for evaluating reactivity of fuel conformers.

The PESs for thermal decomposition of MNB and DNB were characterized at the M06-2X/aug-cc-pVTZ and  $\text{RCCSD(T)}/\text{cc-pV}\infty\text{Z}/\text{M06-2X/aug-cc-pVTZ}$  level of theory. In particular, the values of the energy barriers and endothermicities at the M06-2X/aug-cc-pVTZ level of theory show remarkable agreement with the values obtained from the  $\text{RCCSD(T)}/\text{cc-pV}\infty\text{Z}/\text{M06-2X/aug-cc-pVTZ}$  computations, implying that the former level of theory could be applicable to larger

analogous systems (Figure 24). It was found that the thermal decomposition of MNB is initiated by the elimination of HNCO and HNN(O)OH intermediates. Intramolecular transfer of a H-atom, respectively, from the terminal NH<sub>2</sub> group to the adjacent carbonyl O-atom via a six-member-ring transition state eliminates HNCO with an energy barrier of 35 kcal/mol and from the central NH group to the adjacent nitro O-atom eliminates HNN(O)OH with an energy barrier of 34 kcal/mol. Elimination of HNN(O)OH is also the primary process involved in the thermal decomposition of DNB, which processes C<sub>2v</sub> symmetry. The energy barrier for HNN(O)OH elimination in DNB is 6.60 kcal/mol lower than that in MNB due to an extra hydrogen bond in the transition state for the former, which results in DNB being less stable than MNB. Furthermore, the HNN(O)OH intermediate subsequently decomposes via multiple wells and multiple channels. The RRKM/multi-well master equation simulations revealed that decomposition to thermodynamically stable N<sub>2</sub>O + H<sub>2</sub>O products via isomerization is the primary channel during HNN(O)OH decomposition. The rate coefficients for the primary decomposition channels for MNB and DNB were quantified as functions of temperature and pressure.

The rate coefficient data can be used to interpret the experimental results of Klapötke et al.<sup>17</sup> regarding the thermal stability of MNB and DNB, and their decomposition products and ignition. Such information is essential in the design and manipulation of molecular systems for the development of new energetic materials for advanced propulsion applications.

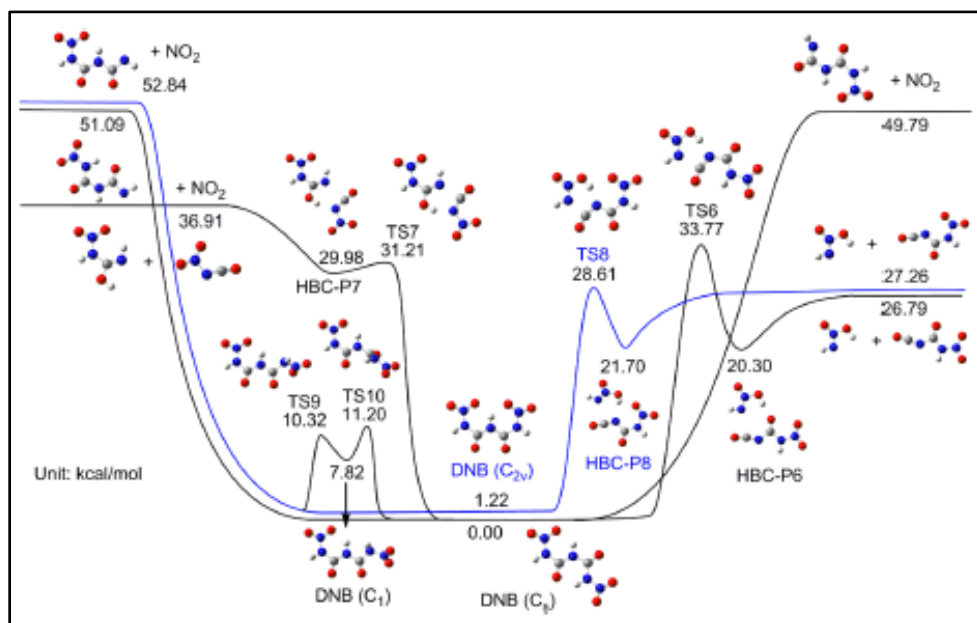


**Figure 24.** The potential energy surface for the thermal decomposition of DNB calculated at the M06-2X/aug-cc-pVTZ level of theory.

### N<sub>2</sub>H<sub>3</sub> + NO<sub>2</sub> reaction kinetics.<sup>18</sup>

The N<sub>2</sub>H<sub>3</sub> + NO<sub>2</sub> reaction plays a key role during the early stages of hypergolic ignition between N<sub>2</sub>H<sub>4</sub> and N<sub>2</sub>O<sub>4</sub>. Here for the first time, the reaction kinetics of N<sub>2</sub>H<sub>3</sub> in excess NO<sub>2</sub> was studied in

2.0 Torr of  $N_2$  and in the temperature range 298–348 K in a pulsed photolysis flow-tube reactor coupled to a mass spectrometer. The temporal profile of the product, HONO, was determined by direct detection of the  $m/z$  +47 ion signal. For each chosen  $[NO_2]$ , the observed [HONO] trace (Figure 25) could be fitted to a bi-exponential kinetics expression, which yielded a value for the pseudo-first-order rate coefficient,  $k'$ , for the reaction of  $N_2H_3$  with  $NO_2$ . The slope of a plot of  $k'$  versus  $[NO_2]$  yielded a value for the total bimolecular rate coefficient, which could be fitted to an Arrhenius expression;  $(2.36 \pm 0.47) \times 10^{-12} \exp((520 \pm 350)/T) \text{ cm}^3 \text{ molecule}^{-1} \text{ s}^{-1}$ . The errors are  $1\sigma$  and include estimated uncertainties in the  $NO_2$  concentration.

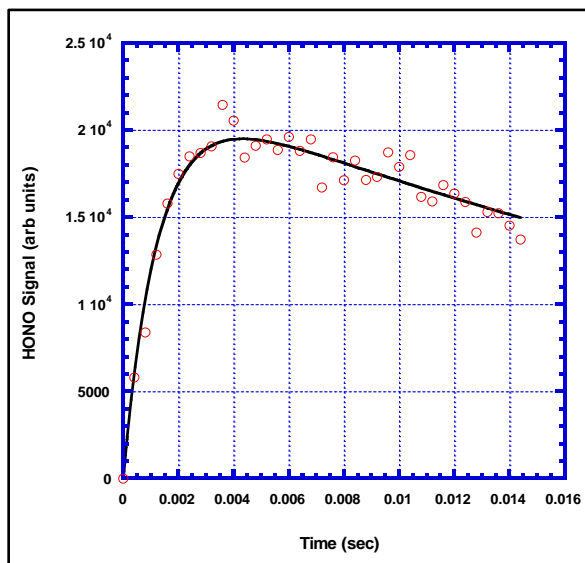


**Figure 25.** Typical [HONO] temporal profile observed in the flow-tube reactor at 298 K.

The potential energy surface of  $N_2H_3 + NO_2$  was investigated by several advanced *ab initio* theories, including coupled-cluster and multi-reference second-order perturbation methods, and the results reveal a new reaction mechanism. The reaction is exothermic by up to 42 kcal/mol, and proceeds via a complex addition-isomerization-dissociation mechanism with the transition state energies of all the reaction channels either below or nearly equal to that of the entrance asymptote, implying all reaction channels are important for products formation.

It was found that the direct addition of  $NO_2$  to one side of  $N_2H_3$ , via a 6-member-ring transition state, forms the adduct,  $N_2H_3NO_2$ , and that addition to the other side of  $N_2H_3$ , via a 5-member-ring transition state, forms a complex that undergoes two facile isomerization reactions to form the adduct,  $N_2H_3ONO$ . The subsequent isomerization and decomposition of the addition adducts lead to various products. The temperature and pressure dependent rate coefficients for all of the isomerization and dissociation channels were computed via RRKM/multi-well master equation simulations (Figure 26). The results reveal that the dominant channels for the  $N_2H_3 + NO_2$  reaction system lead to the formation of the products, trans-HONO + trans-NH=NH, and NO +  $NH_2NHO$ , through the addition adducts  $N_2H_3NO_2$  and  $N_2H_3ONO$ , and these addition adducts show very strong negative temperature dependences in the temperature range from 300 to 3000K.



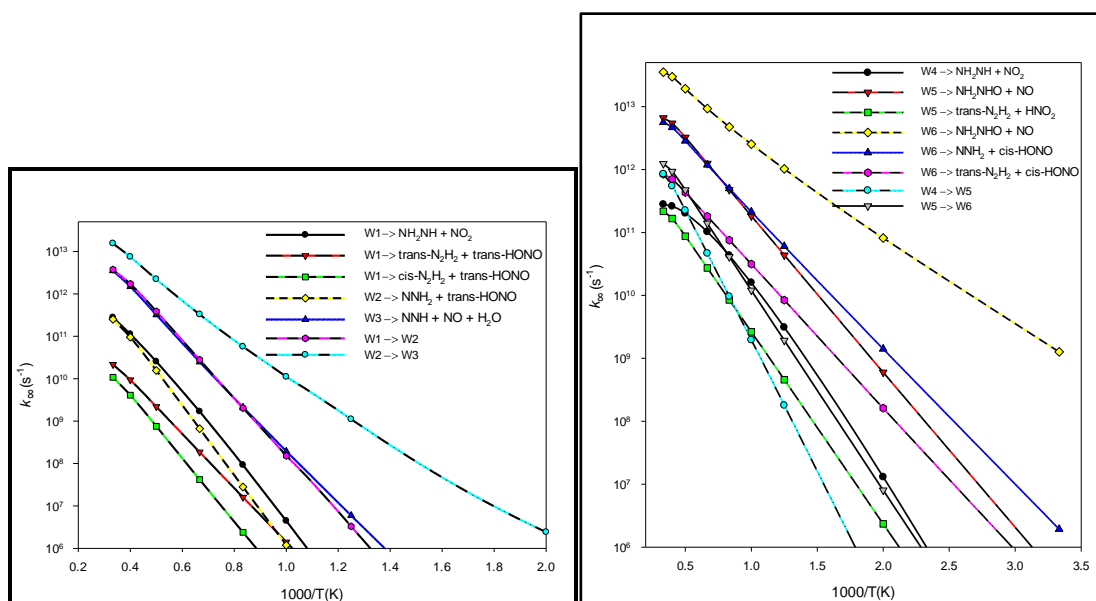


**Figure 26.** High pressure limit rate coefficients for the dissociation and isomerization channels of  $\text{N}_2\text{H}_3 + \text{NO}_2 \rightarrow \text{N}_2\text{H}_3\text{NO}_2 \rightarrow \text{Products}$  (left) and of  $\text{N}_2\text{H}_3 + \text{NO}_2 \rightarrow \text{N}_2\text{H}_3\text{ONO} \rightarrow \text{Products}$  (right).

### Flammability limits.<sup>19</sup>

A numerical method is demonstrated in which a simple flame temperature criterion of 2700 K is used to map out flammability diagrams as a function of total mixture pressure and equivalence ratio in the hypergolic system, monomethylhydrazine/nitrogen tetroxide/helium (MMH/NTO/He). The computed results are in good agreement with experimentally determined ignition diagrams for MMH/NTO/He (Figure 27). The method is used to predict the lower and upper flammability limits of other hypergolic mixtures at 298 K and 1 atm. This numerical method allows for the rapid assessment of the flammability hazards of uncharacterized fuel/oxidant mixtures that may be encountered in the work place as well as their auto-ignitability (hypergolicity) in combustion devices.

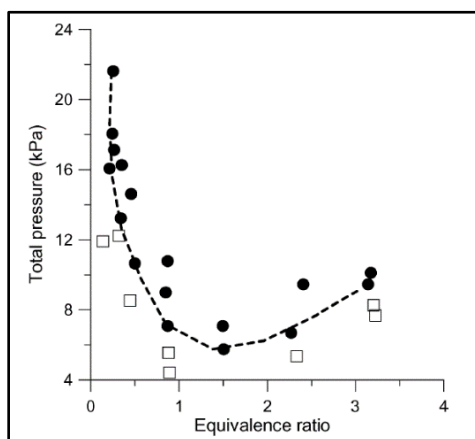


**Figure 27.** MMH/NTO/He (with 60 mol% of He) flammability diagram as a function of total mixture pressure and equivalence ratio obtained by assuming rapid mixing.  $\square$  : no ignition;  $\bullet$  : ignition.

Future work will extend this method to mixtures of ionic liquid fuels with common oxidizers such as HNO<sub>3</sub>, NTO, and H<sub>2</sub>O<sub>2</sub>. This method can be utilized to systematically screen for suitable ionic liquid/oxidizer candidates for potential hypergolic propellant applications provided that the chemical kinetics model for ignition is sufficiently developed to determine temperature profiles to assess that “reasonable” i.e., not too long, ignition delays are expectable.

## Conclusion

In this work we have used a variety of complementary experimental techniques and theoretical approaches to elucidate the reaction mechanisms involved in the decomposition of energetic RTILs as a result of thermolysis, catalysis and oxidation. As our knowledge improves in these areas, it should be possible to build predictive numerical models for the accurate assessment of the performance and the state-of-health in RTIL monopropellant and bipropellant thrusters.

## References Task II

- 10.(a)** Chambreau, S. D.; Schenk, A. C.; Sheppard, A. J.; Yandek, G. R.; Vaghjiani, G. L.; Maciejewski, J.; Koh, C. J.; Golan, A.; Leone, S. R., Thermal Decomposition Mechanisms of Alkylimidazolium Ionic Liquids with Cyano-Functionalized Anions. *The Journal of Physical Chemistry A* **2014**, *118*, 11119-11132; **(b)** Liu, J.; Chambreau, S. D.; Vaghjiani, G. L., Dynamics Simulations and Statistical Modeling of Thermal Decomposition of 1-Ethyl-3-methylimidazolium Dicyanamide and 1-Ethyl-2,3-dimethylimidazolium Dicyanamide. *The Journal of Physical Chemistry A* **2014**, *118*, 11133-11144.
- 11.**Chambreau, S. D.; Koh, C. J.; Popolan-Vaida, D. M.; Gallegos, C. J.; Hooper, J. B.; Bedrov, D.; Vaghjiani, G. L.; Leone, S. R., Flow-Tube Investigations of Hypergolic Reactions of a Dicyanamide Ionic Liquid Via Tunable Vacuum Ultraviolet Aerosol Mass Spectrometry. *The Journal of Physical Chemistry A* **2016**, 10.1021/acs.jpca.6b06289.
- 12.**Chambreau, S. D.; Schneider, S.; Rosander, M.; Hawkins, T.; Gallegos, C. J.; Pastewait, M. F.; Vaghjiani, G. L., Fourier Transform Infrared Studies in Hypergolic Ignition of Ionic Liquids. *The Journal of Physical Chemistry A* **2008**, *112*, 7816-7824.
- 13.**Perez, J. P. L.; Yu, J.; Sheppard, A. J.; Chambreau, S. D.; Vaghjiani, G. L.; Anderson, S. L., Binding of Alkenes and Ionic Liquids to B-H Functionalized Boron Nanoparticles: Creation of Unoxidized Particles with Controlled Dispersibility. *ACS Applied Materials & Interfaces* **2015**, *7*, 9991-10003.
- 14.**Sun, R.; Siebert, M. R.; Xu, L.; Chambreau, S. D.; Vaghjiani, G. L.; Lischka, H.; Liu, J.; Hase, W. L., Direct Dynamics Simulation of the Activation and Dissociation of 1,5-Dinitrobiuret (HDNB). *The Journal of Physical Chemistry A* **2014**, *118*, 2228-2236.
- 15.**Liu, J.; Chambreau, S. D.; Vaghjiani, G. L., Thermal Decomposition of 1,5-Dinitrobiuret (DNB): Direct Dynamics Trajectory Simulations and Statistical Modeling. *The Journal of Physical Chemistry A* **2011**, *115*, 8064-8072.

- 16.** Sun, H.; Vaghjiani, G. L., *Ab initio* Kinetics and Thermal Decomposition Mechanism of Mononitrobiuret and 1,5-Dinitrobiuret. *The Journal of Chemical Physics* **2015**, *142*, 204301-20415.
- 17.** Geith, J.; Holl, G.; Klapötke, T. M.; Weigand, J. J., Pyrolysis Experiments and Thermochemistry of Mononitrobiuret (MNB) and 1,5-dinitrobiuret (DNB). *Combustion and Flame* **2004**, *139*, 358-366.
- 18.** Vaghjiani, G. L.; Sun, H.; Chambreau, S. D.; Schenk, A.; Law, C. K., Experimental and Theoretical Investigations of the Radical-Radical Reaction:  $\text{N}_2\text{H}_3 + \text{NO}_2$ , *The Journal of Physical Chemistry A* **2016**, in preparation.
- 19.** Sabard, J.; Catoire, L.; Chambreau, S. D.; Vaghjiani, G. L., Predicting Hypergolic Mixture Flammability Limits: Application for Non-ionic Liquid Based Systems, *Combustion and Flame*, **2016**, submitted.

### 3.0 Publication

#### Published in Peer Reviewed Journals, Books, etc:

- 1) Vaghjiani, G. L.; Sun, H.; Chambreau, S. D.; Schenk, A.; Law, C. K., Experimental and Theoretical Investigations of the Radical-Radical Reaction:  $\text{N}_2\text{H}_3 + \text{NO}_2$ , *The Journal of Physical Chemistry A* **2016**, in preparation.
- 2) Sabard, J.; Catoire, L.; Chambreau, S. D.; Vaghjiani, G. L., Predicting Hypergolic Mixture Flammability Limits: Application for Non-ionic Liquid Based Systems, *Combustion and Flame*, **2016**, submitted
- 3) Chambreau, S. D.; Koh, C. J.; Popolan-Vaida, D. M.; Gallegos, C. J.; Hooper, J. B.; Bedrov, D.; Vaghjiani, G. L.; Leone, S. R., Flow-Tube Investigations of Hypergolic Reactions of a Dicyanamide Ionic Liquid Via Tunable Vacuum Ultraviolet Aerosol Mass Spectrometry. *The Journal of Physical Chemistry A* **2016**, 10.1021/acs.jpca.6b06289.
- 4) Sun, H.; Vaghjiani, G. L., *Ab initio* Kinetics and Thermal Decomposition Mechanism of Mononitrobiuret and 1,5-Dinitrobiuret. *The Journal of Chemical Physics* **2015**, *142*, 204301-20415
- 5) "Binding of Alkenes and Ionic Liquids to B-H-Functionalized Boron Nanoparticles: Creation of Particles with Controlled Dispersibility and Minimal Surface Oxidation," J. 4) P. L. Perez, J. Yu, A. J. Sheppard, S. D. Chambreau, G. L. Vaghjiani, and S. L. Anderson, *ACS Appl. Mater. Interfaces*, **2015**, *7* (18), 9991–10003. DOI: 10.1021/acsami.5b02366
- 6) "Boron Nanoparticles with High Hydrogen Loading: Mechanism for B-H Binding and Potential for Improved Combustibility and Specific Impulse" Jesus Paulo L. Perez, Brandon W. McMahon, Jiang Yu, Stefan Schneider, Jerry A. Boatz, Tom W. Hawkins, Parker D. McCrary, Luis A. Flores, Robin D. Rogers, Scott L. Anderson, *Appl. Mater. Interfaces*, **2014**, *6* (11), 8513–8525.
- 7) "Direct Dynamics Simulation of the Activation and Dissociation of the Ionic Liquid 1,5-Dinitrobiuret (DNB)" Rui Sun, Matthew R Siebert, Lai Xu, Steven D. Chambreau, Ghanshyam L. Vaghjiani, Hans Lischka, Jianbo Liu, and William Louis Hase, *Journal of Physical Chemistry A* **2014** DOI: 10.1021/jp5002622
- 8) "Thermal Decomposition Mechanisms of Alkylimidazolium Ionic Liquids with Cyano-Functionalized Anions" Steven D. Chambreau, Adam C. Schenk, Anna J. Sheppard, Gregory R. Yandek, Ghanshyam L. Vaghjiani, John Maciejewski, Christine J. Koh, Amir Golan and Stephen R. Leone, *Journal of Physical Chemistry A*, **2014** *118* (47), 11119–11132, DOI: 10.1021/jp5095855
- 9) "Dynamics Simulations and Statistical Modeling of Thermal Decomposition of 1-Ethyl-3-methylimidazolium Dicyanamide and 1-Ethyl-2,3-dimethylimidazolium Dicyanamide" Jianbo Liu, Steven D. Chambreau, and Ghanshyam L. Vaghjiani, *Journal of Physical Chemistry A*, **2014** *118* (47), 11133–11144, DOI: 10.1021/jp5095849
- 10) "Helium Nanodroplet Isolation and Infrared Spectroscopy of the Isolated Ion-Pair 1-Ethyl-3-methylimidazolium bis(trifluoromethylsulfonyl)imide" Emmanuel I. Obi, Christopher M. Leavitt, Paul L. Raston, Christopher P. Moradi, Steven D. Flynn, Ghanshyam L. Vaghjiani, Jerry

A. Boatz, Steven D. Chambreau, and Gary E. Douberly, *J. Phys. Chem. A*, **2013**, 117 (37), 9047–9056.

#### **Invention Disclosures and Patents Granted:**

- 1 “Green hypergolic fuels,” Hawkins, Tommy W.; Schneider Stefan; Rosander, Michael; Hudgens Leslie U.S. (2015), US9090519

Provided is an ionic liquid (IL) having anions and cations with a metalohydride in the IL of borohydrides and/or aluminum hydrides, as a fuel and a choice of one or more oxidizers, which fuel and oxidizer have hypergolic tendencies.

- 2 “Catalytic hypergolic bipropellants,” Schneider, Stefan; Hawkins, Tommy W.; Ahmed, Yonis; Rosander, Michael U.S. (2014), US 8758531

Provided is a fuel of catalytic metal-contg. ionic liq. (MCIL) and an IL, to spur hypergolic ignition of such liqs. upon contact with an oxidizer to define a hypergolic bipropellant.

- 3 “Bipropellants based on chosen salts,” Schneider, Stefan; Hawkins, Tommy W.; Ahmed, Yonis; Rosander, Michael U.S. (2014), US 8758531

Advanced bipropellant fuels with fast ignition upon mixing with storable oxidizer (N2O4 , nitric acid) have been synthesized and demonstrated. The bipropellant fuels are based upon salts containing dicyanamide or tricyanomethanide anions and employ at least two hydrazine functionalities in the cations.

#### **Invited Lectures, Presentations, Talks, etc:**

“5-(Azido-alkyl)-1H-tetrazole: Synthesis and characterization,” Yonis Ahmed, Christina Gibson, Stefan Schneider, Stephan Deplazes presented at 251st ACS National Meeting & Exposition, San Diego, CA, United States, March 13-17, 2016.

“Sodium borohydride amine complexes: A simple way to organic borohydride salts,” Stefan Schneider, Yonis Ahmed, Stephan Deplazes, Christina Gibson presented at 251st ACS National Meeting & Exposition, San Diego, CA, United States, March 13-17, 2016.

“Lithium Borohydride Complexes of Tetrazole Derivatives,” Stephan Deplazes, Stefan Schneider, Yonis Ahmed, Christina Gibson and Cpt. Andrew Beauchamp presented at 251st ACS National Meeting & Exposition, San Diego, CA, United States, March 13-17, 2016.

“Improving Performance in Energetic Ionic Liquid-Based Propulsion Systems,” S. D. Chambreau, G. L. Vaghjani, S. R. Leone, and S. L. Anderson. Poster presented at the 2015 Air Force Office of Scientific Research Molecular Dynamics Contractors Meeting, May 18-21, 2015 Kirtland AFB, Albuquerque, NM.

"Theoretical and Experimental Studies on the Radical-Radical Reaction:  $\text{NO}_2 + \text{N}_2\text{H}_3$ ," G. L. Vaghjiani, H. Sun, S. D. Chambreau, and A. Schenk. Poster presented at the 2015 Air Force Office of Scientific Research Molecular Dynamics Contractors Meeting, May 18-21, 2015 Kirtland AFB, Albuquerque, NM.

"Recent advances in understanding the reactivity of energetic ionic liquids in propulsion applications," Steven D. Chambreau, Ghanshyam L. Vaghjiani, Timothy K. Minton, Stephen R. Leone, poster presented at Air Force Office of Scientific Research Molecular Dynamics Contractors review meeting, Arlington, VA, May 19, 2014.

"Advances in Understanding the Ignition of Ionic Liquid Propellants," Steven D. Chambreau, invited presentation at 6.1 Review, Antelope Valley College, January 28, 2014.

"Recent advances in understanding the reactivity of energetic ionic liquids in propulsion applications," Steven D. Chambreau, Ghanshyam L. Vaghjiani, Timothy K. Minton, Stephen R. Leone, talk presented at the American Chemical Society Annual Fall Meeting, San Francisco, CA, August 12, 2014.

"Synthesis of novel hydrazine tethered ionic liquids," Beauchamp, Andrew; Deplazes, Stephan; Ahmed, Yonis; Franquera, Christina; Schneider, Stefan, presented at 248th ACS National Meeting & Exposition, San Francisco, CA, United States, August 10-14, 2014.

"Synthesis and characterization of 5-(hydrazino-alkyl) tetrazoles," Ahmed, Yonis; Beauchamp, Andrew; Deplazes, Stephan; Franquera, Christina; Schneider, Stefan, presented at 248th ACS National Meeting & Exposition, San Francisco, CA, United States, August 10-14, 2014.

"Catalytic ignition of ionic liquid fuels by ionic liquids," Schneider, Stefan; Deplazes, Stephan; Ahmed, Yonis; Beauchamp, Andrew; Franquera, Christina, presented at 248th ACS National Meeting & Exposition, San Francisco, CA, United States, August 10-14, 2014.

"Novel coordination chemistry of aluminum borohydride," Deplazes, Stephan; Schneider, Stefan; Ahmed, Yonis; Franquera, Christina; Beauchamp, Andrew, presented at 248th ACS National Meeting & Exposition, San Francisco, CA, United States, August 10-14, 2014.

#### **Honors Received (include lifetime honors such as Fellow, Honorary Doctorates, etc):**

Dr. Schneider was bestowed the competitive **General Benjamin D. Foulois Award**. This award is given for significant and outstanding in-house science of importance to the Air Force. This award recognizes a culmination, multi-year outstanding achievement. Air Force Research Laboratory, Edwards AFB, CA, Jan 2014.

#### **Extended Scientific Visits From and To Other Laboratories:**

Dr. Chambreau traveled to the Advanced Light Source at Lawrence Berkeley National Laboratory to perform experiments using X-ray microtomography to investigate the thermal degradation of monopropellant catalysts at high temperatures: October 6-11, **2015**.

Dr. Chambreau traveled to Stanford University to perform experiments using nanotip ambient ionization mass spectrometry to investigate the catalytic reactivity of ionic liquid monopropellants: October 12-13, **2015**.

Dr. Chambreau traveled to Stanford University to perform experiments using desorption electrospray ionization mass spectrometry to investigate the catalytic reactivity of ionic liquid monopropellants: August 14-19, **2014**.

Dr. Chambreau traveled to the Advanced Light Source at Lawrence Berkeley National Laboratory to perform ongoing experiments using tunable vacuum ultraviolet photoionization time of flight spectrometry to probe the catalytic reactivity of aerosolized ionic liquid monopropellants, August 19-26, **2014**.

Dr. Chambreau traveled to Berkeley, CA to perform experiments at the Chemical Dynamics Beamline at the Advanced Light Source (Lawrence Berkeley National Laboratory), December 3-11, **2013**.

#### **4.0 Appendix A: In-house Activities**

##### **Personnel:**

###### **Air Force Civilian:**

J. D. Mills, Ph.D., Chemist (50%)  
G. L. Vaghjiani, Ph.D., Chemist (20%)  
S. Schneider, Ph.D., Chemist (70%)  
S. Deplazes, Ph.D., Chemist (90%)  
J. Boatz, Ph.D., Chemist (10%)

###### **On-site Contractor:**

Yonis Ahmed, Ph.D., Chemist (100%)  
S. D. Chambreau, Ph.D., Chemist (100%)  
C. Gibson, B.Sc., Chemist (100%)

###### **Air Force Military:**

Lt. A. Sheppard, B.Sc., Aerospace Eng. (30%)  
Capt. A. Beauchamp, M.Sc., Chemist (50%)  
Lt. T. Schulmeister, B.Sc., Physics. (30%)



## Appendix B: Technology Assists, Transitions, or Transfers

Task Title	Performance Period	AFOSR Program Manager	TD Performer	Customer	Research Result	Application	From	To	Application
IONIC LIQUID-BASED PROPELLANTS	10/2012-9/2015	BERMAN	USAF-AFRL Brand	NASA	Providing advanced monopropellant based on AFOSR material for spacecraft demonstration	Spacecraft Monopropulsion	L,I	O	Pd
IONIC LIQUID-BASED PROPELLANTS	6/2012-12/2014	BERMAN	USAF-AFRL Brand	Aerojet	Providing advanced monopropellants based on AFOSR material for ACS demonstration	Attitude control for missiles	L	I	Pd
IONIC LIQUID-BASED PROPELLANTS	10/2010-9/2016	BERMAN	USAF-AFRL (CFD RESEARCH CORP., HUNTSVILLE, AL, Contract FA9300-11-C-3004), Vaghjiani	DoD	Development of software for prediction of ignition delays for energetic ionic liquids. Phase-II stage of development. Also, making energetic IL propellants that complement AFOSR efforts.	Advanced Liquid Rocket Engines	L	I	Pd
IONIC LIQUID-BASED PROPELLANTS	10/2010-10/2014	BERMAN	USAF-AFRL (WASATCH MOLECULAR INC., SALT LAKE CITY, UT, Contract FA9300-11-C-3012), Vaghjiani	DoD	Development of software for prediction of ignition delays for energetic ionic liquids. Phase-II stage of development. Complements AFOSR & EOARD IL ignition M&S efforts.	Advanced Liquid Rocket Engines	L	I	Pd
IONIC LIQUID-BASED PROPELLANTS	8/2012-5/2017	BERMAN	USAF-AFRL (ULTRAMET, PACOIMA, CA Contract FA9300-12-C-2003), Vaghjiani & Zuttarelli	DoD	Modeling the decomposition of HAN-based monopropellants and associated catalysts. Phase-II stage of development. Complements AFOSR energetic IL propellant decomposition efforts.	Advanced Liquid Rocket Engines	L	I	Pd
IONIC LIQUID-BASED PROPELLANTS	6/2016-12/2018	BERMAN	USAF-AFRL (CFD RESEARCH CORP., HUNTSVILLE, AL, Vaghjiani		Development of software for prediction of ignition delays for energetic ionic liquids. Procurement stage of development. Also, making energetic IL propellants that complement AFOSR efforts.	Advanced Liquid Rocket Engines	L	AF	Pd

Note: In each of the last three columns, enter the appropriate codes from the lists below:

Transitioned From:

AFRL = L; Industry = I; Academia = A

Transitioned To:

Industry = I; Air Force 6.2 or 6.3 = AF; Other AF, DoD, Government, etc. = O (please specify)

Application:

Product (New or Improved) = Pd; Process (New or Improved) = Pc; Other = O (please specify)

Distribution A: Approved for Public Release; Distribution unlimited

This Page Intentionally Left Blank

**AFRL-RQ-ED-TR-2016-0025**

**Primary Distribution of this Report:**

RQR  
AFRL R&D Case Files  
Completed Interim and Final Tech Reports Repository

AFRL/RQ Technical Library (2 CD + 1 HC)  
6 Draco Drive  
Edwards AFB, CA 93524-7130

Johns Hopkins University  
Whiting School of Engineering  
ATTN: Mary T. Gannaway/FSO  
10630 Little Patuxent Pkwy, Suite 202  
Columbia, MD 21044-3286

Defense Technical Information Center  
(1 Electronic Submission via STINT)  
Attn: DTIC-ACQS  
8725 John J. Kingman Road, Suite 94  
Ft. Belvoir, VA 22060-6218